

SMR 1232 - 24

**XII WORKSHOP ON
STRONGLY CORRELATED ELECTRON SYSTEMS**

17 - 28 July 2000

Hidden Order in URu₂Si₂

Studied by High-Pressure Experiments

H. AMITSUKA
Hokkaido University - Dept. of Physics
060 0810 Sapporo, Japan

These are preliminary lecture notes, intended only for distribution to participants.

Pressure-Induced Magnetic Phase Transition of the 5f Electron System URu_2Si_2

Hiroshi AMITSUKA*, Makoto YOKOYAMA, Kenichi TENYA, Toshiro SAKAKIBARA,
Keitaro KUWAHARA¹, Masugu SATO², Naoto METOKI², Tetsuo HONMA², Yoshichika ÔNUKI^{2,3},
Shuzo KAWARAZAKI³, Yoshihito MIYAKO³, Srinivasan RAMAKRISHNAN⁴, and John A. MYDOSH⁵

Graduate School of Science, Hokkaido University, Sapporo 060-0810, Japan

¹*Department of Physics, Tokyo Metropolitan University, Hachioji, Tokyo 192-0397, Japan*

²*Advanced Science Research Center, Japan Atomic Energy Research Institute, Ibaraki 319-1195, Japan*

³*Graduate School of Science, Osaka University, Toyonaka 560-0043, Japan*

⁴*Condensed Matter Group, Tata Institute of Fundamental Research, Mumbai 400 005, India*

⁵*Kamerlingh Onnes Laboratory, Leiden University, PO Box 9504, 2300 RA Leiden, The Netherlands*

(Received December 28, 1999)

A puzzling phase transition at $T_0 \sim 17.5$ K of the heavy-electron 5f system URu_2Si_2 is characterized by development of an unusually small staggered moment μ_0 concomitant with large bulk anomalies and sharp magnon excitations. Through elastic and inelastic neutron scattering, we have studied the influence of pressure P up to ~ 2.8 GPa on this phase transition. For pressures less than 1.3 GPa, μ_0 at 1.4 K is quasi-linearly enhanced from $\sim 0.017(3) \mu_B$ to $\sim 0.25(2) \mu_B$, while its onset temperature increases only ten percent. We have also observed a sharp phase transition at $P_c \sim 1.5$ GPa, above which a 3D-Ising type of antiferromagnetic phase ($\mu_0 \sim 0.4 \mu_B$) appears. Sharp magnon excitations at $Q = (1,0,0)$ and $(1,0.4,0)$ collapse in this high- P phase. The lattice parameter a decreases discontinuously at P_c even for $T > T_0$, indicating that pressure induces a significant change in electronic states in a higher characteristic energy scale. We show that the observed magnetic instability could qualitatively well be explained by competition between quadrupolar and dipolar interactions in a non-trivial Γ_8 doublet.

KEYWORDS: URu_2Si_2 , tiny magnetic moment, neutron scattering, high pressure

§1. Introduction

The ternary intermetallic compound URu_2Si_2 is a well-known heavy-electron system in that 5f electrons clearly undergo two successive phase transitions at ~ 17.5 K and ~ 1 K.¹⁻⁴⁾ It crystallizes in the body-centered tetragonal ThCr_2Si_2 structure with space group of $I4/mmm$. The 1K transition is known as the onset of unconventional superconductivity due to heavy quasi-particles, while the origin of the 17.5 K transition is still in controversy in spite of intensive studies for the past fifteen years.

Microscopic studies of neutron scattering⁵⁻⁷⁾ and X-ray magnetic scattering⁸⁾ have revealed a type-I antiferromagnetic modulation with 5f magnetic dipoles polarized along the c axis developing below about 17.5 K. The magnitude of the staggered moment μ_0 is estimated to be ~ 0.02 – $0.04 \mu_B/\text{U}$, which is extremely small compared with the effective moment ($\sim 3 \mu_B$) estimated from the high-temperature magnetic susceptibility.^{1,2)} The similar tiny-moment state has been reported for UPt_3 ⁹⁾ and CeRh_2Si_2 (under high pressure),¹⁰⁾ but URu_2Si_2 is unique in the following two respects.

First, the development of μ_0 is accompanied by disproportionately large bulk anomalies.¹⁻⁴⁾ For example, the specific-heat jump ($\Delta C/T \sim 300 \text{ mJ/K}^2\text{mol}$) at 17.5 K involving a large reduction of the 5f entropy ($S \sim 0.2R \ln 2$) cannot simply be reproduced by the one-

present condensation of the 5f moments.¹¹⁾ Secondly, an energy gap occurs in the density of states in the ordered state. This is indicated by a term, $\exp(-\Delta/T)$, appearing in various macroscopic quantities such as resistivity¹²⁾ and specific heat,³⁾ and also manifested in measurements of neutron scattering,¹³⁾ far-infrared reflectance,¹⁴⁾ and tunneling spectroscopy.¹⁵⁾ The evaluated gap averages ~ 100 K.

In the neutron scattering, the excitations are observed as spin waves which are polarized along the c -axis with a large dipolar matrix element of $\mu_z^{\text{ex}} \equiv g\mu_B |\langle 0|J_z|1 \rangle| \sim 1.2$ – $1.8 \mu_B$.^{5,6)} The inelastic reflections are particularly strong at $Q = (1,0,0)$ and $(1,0.4,0)$, where the dispersion curve takes minima with gap energies of $\Delta_{(1,0,0)} \sim 2.0$ meV and $\Delta_{(1,0.4,0)} \sim 4.1$ meV. In the paramagnetic state, on the other hand, the system shows a broad continuous spectrum of antiferromagnetically correlated spin fluctuations. The fluctuating moment is large, comparable to μ_z^{ex} , and the corresponding staggered susceptibility diverges as the system approaches the phase transition.¹⁶⁾ However, the quasi-elastic peak seen just above 17.5 K does not grow into an adequate Bragg peak, but turns into the above magnon spectrum.

To explain the unusual features of the phase transition, various scenarios have been proposed, which can be classified into two groups: (i) the transition is uniquely caused by magnetic dipoles with highly reduced g -values,¹⁷⁻¹⁹⁾ and (ii) there is hidden order of a non-dipolar degree of freedom.²⁰⁻²⁷⁾ Staggered quadrupolar

* E-mail: amiami@phys.sci.hokudai.ac.jp

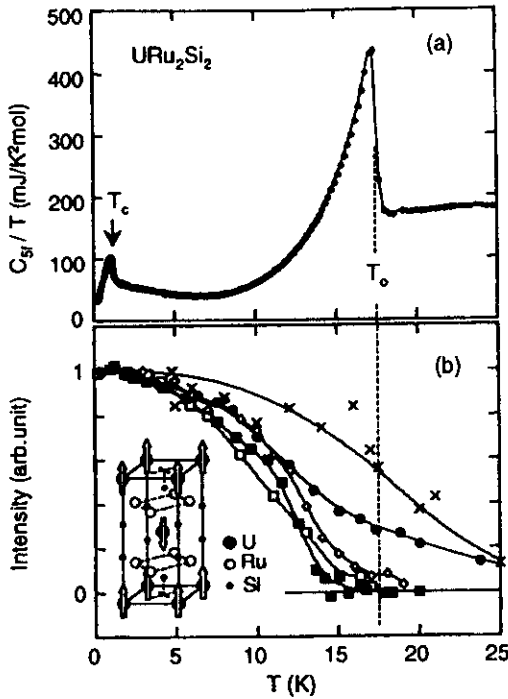


Fig. 1. (a) The 5f-electronic specific heat C_{5f}/T of a polycrystal of URu_2Si_2 annealed at 800 °C for one month. Non-5f contribution was subtracted by using the data of $ThRu_2Si_2$. Presence of two phase transitions are clearly indicated by jumps in the C_{5f}/T curve. Transition temperatures are evaluated as $T_c \sim 1.1$ K and $T_0 \sim 17.5$ K, if they are defined by the midpoints of the jumps. It is known from previous macroscopic measurements that T_0 is hardly affected by sample quality and by annealing conditions. The lowest value of T_0 is reported to be ~ 17 K²⁾ for a polycrystalline sample. (b) Temperature variations of integrated intensity of the type-I antiferromagnetic Bragg peak for a high-purity single crystal (\square) from Mason *et al.*,⁶⁾ and for single crystals annealed at 950–1000 °C for 7–8 days (\bullet , \circ , \blacksquare) from Broholm *et al.*,⁵⁾ Pák *et al.*,²⁸⁾ and Honma *et al.*,⁴⁸⁾ respectively. Temperature variations of the μ SR relaxation rate (\times) for a polycrystalline sample⁴⁹⁾ are also shown. The lines are guides to the eye.

order is believed to be one of the most promising scenarios for the hidden order, which was first suggested by Miyako and his colleagues on the basis of non-linear susceptibility measurements.²⁰⁾ After their definition, we use a notation T_0 to express the transition temperature determined from macroscopic measurements. Three-spin order,²¹⁾ singlet orderings,²⁵⁾ uranium-pair distortions²⁶⁾ and d-type spin density waves²⁷⁾ have also been argued. The models of the second group ascribe the observed tiny moment to side effects, such as secondary order, dynamical fluctuations and coincidental order of a parasitic phase. Each of the dipolar states may have its own energy scale, and to take account of this possibility we define T_m as the onset temperature of μ_0 , distinguishing it from T_0 .

To solve the problem, it is necessary to see how μ_0 relates to the macroscopic anomalies. In contrast to the mean-field-like anomaly of the bulk properties at T_0 , re-

ported T variations of μ_0 differ largely from each other, as typically illustrated in Fig. 1. A recent comparison of T_0 and T_m for the same sample has revealed that T_m becomes lower than T_0 in the absence of annealing.²⁸⁾ In addition, careful high-field studies^{16, 29–31)} have suggested that T_0 and μ_0 are not scaled by a unique function of field. Moreover, ^{29}Si -NMR measurements have never detected the internal fields caused by the development of μ_0 .^{32, 33)} These experimental results seem to support the hidden-order hypotheses.

To further investigate the relation between the tiny moments and the macroscopic anomalies, we have performed neutron scattering experiments under high pressure up to 2.8 GPa. Previous measurements of resistivity and specific heat in P up to 8 GPa have shown that the ordered phase is slightly stabilized by pressure, with a rate of $dT_0/dP \sim 1.3$ K/GPa.^{34–39)} We now show that pressure dramatically increases μ_0 and causes a new phase transition which is accompanied by collapse of the magnetic excitations. We have previously made a brief report on the elastic scattering.⁴⁰⁾ In this paper, we give the detailed description on the experiments and analyses, including the results of inelastic scattering.

§2. Sample and Experimental Technique

The measurements were made on a 8-mm-long approximately cylindrical single crystal with a diameter of 5 mm, grown by the Czochralski technique in a tri-arc furnace in Osaka University. The crystal was annealed at 1000 °C for one week in a vacuum sealed quartz tube. Pressure was applied by means of a barrel-shaped piston cylinder device⁴¹⁾ at room temperature, which was then cooled in a 4He cryostat for temperatures between 1.4 K and 300 K. A solution of Fluorinert 70 and 77 (Sumitomo 3M Co. Ltd., Tokyo) of equal ratio served as the quasihydrostatic pressure transmitting medium. The pressure was monitored by measuring the lattice constant of NaCl, which was encapsulated together with the sample.

The present neutron-scattering experiments were performed on the triple-axis spectrometer TAS-1 at the JRR-3M reactor of Japan Atomic Energy Research Institute. Vertically bent pyrolytic graphite PG(002) crystals were used as a monochromator and an analyzer. Elastic scans were made by using neutrons with a wavelength of $\lambda = 2.3551$ Å, and a 40'–80'–40'–80' horizontal collimation. Higher-order contamination was suppressed with double 4-cm-thick pyrolytic graphite (PG) filters as well as a 4-cm-thick Al_2O_3 filter. The scans were performed in the (h k 0) scattering plane, particularly on the antiferromagnetic Bragg reflections (100) and (210), and on the nuclear ones (200), (020) and (110). For inelastic scattering measurements, we made constant- Q scans at $Q = (1,0,0)$ and $(1,0.4,0)$, using neutrons with a fixed incident energy of $E_0 = 14.7$ meV and a horizontal collimation of (open)–80'–40'–80'. The energy resolution, determined from the vanadium incoherent scattering, was ~ 0.95 meV (FWHM).

The lattice constant a of our sample at 1.4 K at ambient pressure is 4.13(1) Å, which is in good agreement with previous reports.^{5, 16)} Radial scans at (200) and (110) show a crystal mosaic spread of $\sim 20'$ at $P = 0$,

which increases to $\sim 40^\circ$ by applying pressure.

§3. Experimental Results

In Fig. 2, we plot the pressure variations of elastic scans at 1.4 K along the $(1 + \zeta, 0, 0)$ and $(1, \zeta, 0)$ directions around the (100) antiferromagnetic Bragg peak. The instrumental background and the higher-order contributions of nuclear reflections were determined by scans at 35 K and subtracted from the data. The (100) reflection develops rapidly as pressure increases. No other peaks were found in a survey along the principle axes of the first Brillouin zone: $(\zeta, \zeta, 0)$ and $(\zeta, 1 - \zeta, 0)$ for $0.5 \leq \zeta \leq 1$ and $(1, \zeta, 0)$ for $0 \leq \zeta \leq 1$. In addition, the intensities of (100) and (210) reflections follow the $|Q|$ dependence expected from the U⁴⁺ magnetic form factor⁴²⁾ by taking the polarization factor unity. These ensure that the type-I antiferromagnetic structure at $P = 0$ is unchanged by the application of pressure.

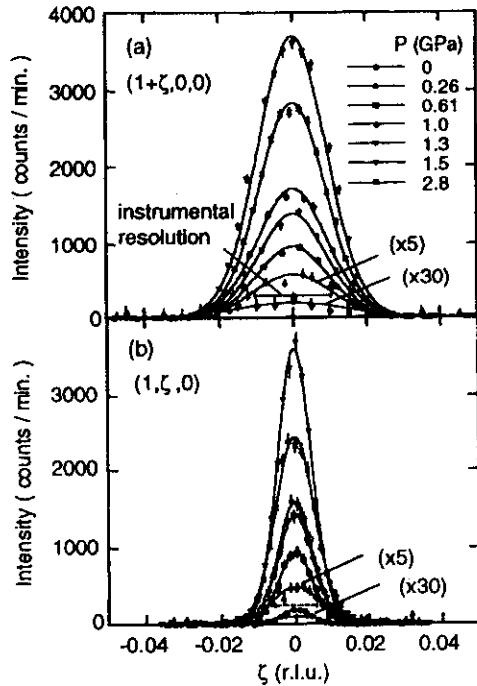


Fig. 2. Pressure variations of line shape at 1.4 K of the (100) antiferromagnetic response in URu₂Si₂ shown in scans along the $(1 + \zeta, 0, 0)$ (a) and $(1, \zeta, 0)$ (b) directions. Widths (FWHM) of the scans taken without filters are shown by horizontal bars as a measure of the instrumental resolution. The resolution is unchanged by applying pressure in the longitudinal scans, while broaden in the vertical scans because of an increase of the crystal mosaic (given by the broken line for $P > 0$).

The widths (FWHM) of the (100) peaks for $P = 0$ and 0.26 GPa are significantly larger than the instrumental resolution ($\sim 0.021(1)$ reciprocal-lattice units for the a^* direction), which was measured by $\lambda/2$ scattering from the nuclear (200) Bragg reflection. From the best fit to the data by a Lorentzian function convoluted with the Gaussian resolution function, the correlation length

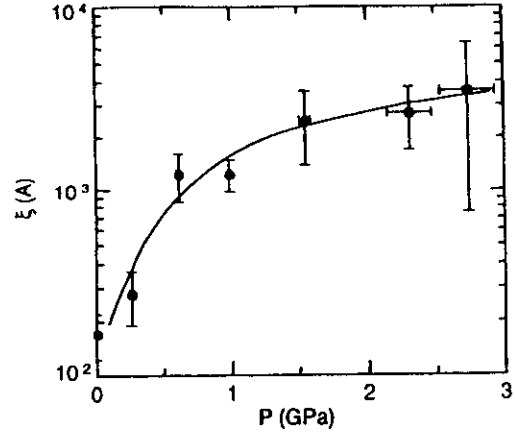


Fig. 3. Pressure dependence of the correlation length along the a^* direction obtained by fitting the (100) peaks with a Lorentzian function convoluted with a Gaussian resolution function.

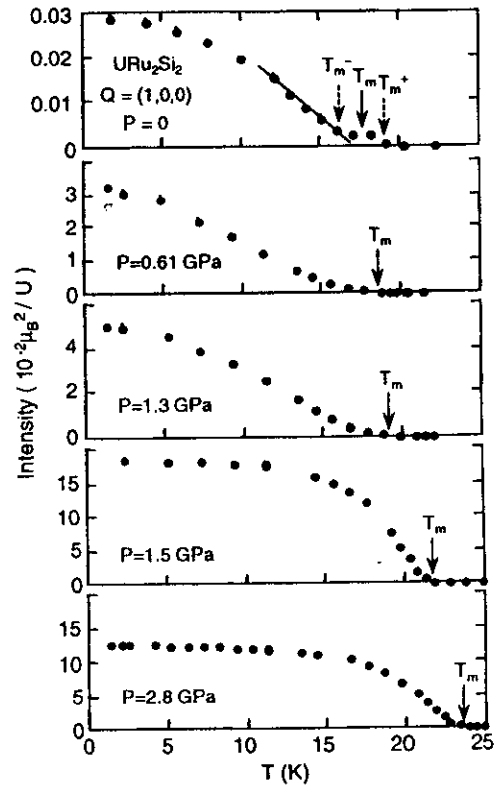


Fig. 4. Temperature dependence of integrated intensity of the (100) Bragg reflection of URu₂Si₂ for several pressures.

ξ along the a^* direction is estimated to be about 180 Å at $P = 0$ and 280 Å at 0.26 GPa. For the higher pressures $P \geq 0.61$ GPa, the simple fits give $\xi > 10^3$ Å, indicating that the line shapes are resolution limited (Fig. 3).

The temperature dependence of the integrated intensity $I(T)$ at (100) varies significantly as P traverses 1.5 GPa ($\equiv P_c$) (Fig. 4). For $P < P_c$, the onset of $I(T)$ is

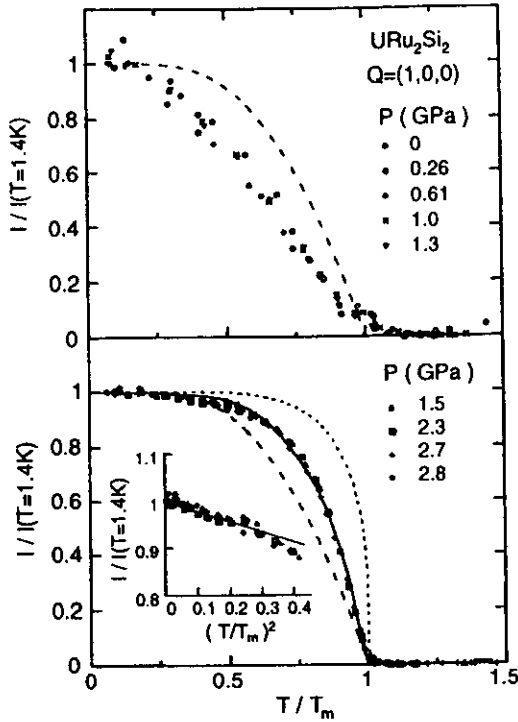


Fig. 5. Normalized intensities $I/I(1.4\text{K})$ plotted as a function of T/T_m for $P < P_c$ (top) and $P > P_c$ (bottom). Theoretical calculations based on 2D,⁵⁰⁾ 3D⁴³⁾ and mean-field Ising models are also given by dotted, solid and broken lines. The inset plots $I/I(1.4\text{K})$ versus $(T/T_m)^2$ at low temperatures. The thin line is a guide to the eye.

not sharp: $I(T)$ gradually develops at a temperature T_m^+ , which is higher than T_0 , and shows a T -linear behavior below a lower temperature T_m^- . Here we empirically define the “antiferromagnetic transition” temperature T_m by the midpoint of T_m^+ and T_m^- . The range of the rounding, $\delta T_m \equiv T_m^+ - T_m^-$, is estimated to be 2–3 K, which is too wide to be usual critical scattering. Above P_c , on the other hand, the transition becomes sharper ($\delta T_m < 2$ K), accompanied by an abrupt increase in T_m at P_c .

If $I(T)$ is normalized to its value at 1.4 K, it scales with T/T_m for various pressures on each side of P_c (Fig. 5). This indicates that two homogeneously ordered phases are separated by a (probably first-order) phase transition at P_c . The growth of $I(T)$ for $P < P_c$ is much weaker than that expected for the mean-field Ising model, showing an unusually slow saturation of the staggered moment. On the other hand, the overall feature of $I(T)$ for $P > P_c$ is approximately described by a 3D-Ising model.⁴³⁾ In the low temperature range $T/T_m < 0.5$, however, $I(T)$ rather follows a T^2 function (the inset of Fig. 5), indicating a presence of gapless collective excitations.⁴⁴⁾

In Fig. 6, we plot the pressure dependence of μ_0 , T_m and the lattice constant a . The magnitude of μ_0 at 1.4 K is obtained through the normalization of the integrated intensity at (100) with respect to the weak nuclear Bragg

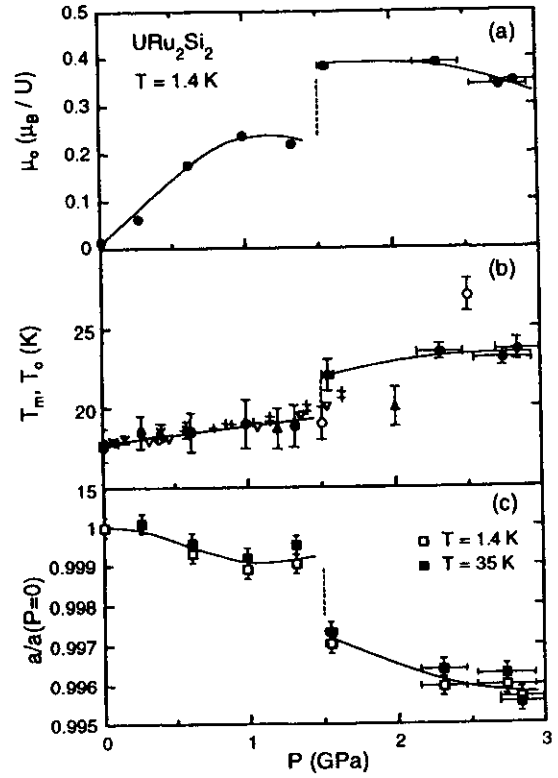


Fig. 6. Pressure variations of (a) staggered magnetic moment μ_0 at 1.4 K; (b) the onset temperature T_m of the moment determined from this work (\bullet) and the transition temperature T_0 determined from resistivity (\diamond ,³⁴⁾ ∇ ,³⁵⁾ \triangle ,³⁷⁾ $+$,³⁸⁾ \circ ,³⁹⁾) and specific heat (\times ³⁰⁾); and (c) the relative lattice constant $a(P)/a(0)$ at 1.4 K and 35 K. T_m is defined by $(T_m^+ + T_m^-)/2$ (see the text), and the range $\delta T_m (\equiv T_m^+ - T_m^-)$ is shown by using error bars. The lines are guides to the eye.

peak at (110). The variation of the (110) intensity with pressure is small ($< 5\%$) and independent of the crystal mosaic, so that the influence of extinction on this reference peak is negligible. μ_0 at $P = 0$ is estimated to be about $0.017(3) \mu_B$, which is slightly smaller than the values (~ 0.02 – $0.04 \mu_B$) of previous studies,^{5, 6, 8, 28)} probably because of a difference in the selection of reference peaks. As pressure is applied, μ_0 increases linearly at a rate $\sim 0.25 \mu_B/\text{GPa}$, and shows a tendency to saturate at $P \sim 1.3$ GPa. Around P_c , μ_0 abruptly increases from $0.23 \mu_B$ to $0.40 \mu_B$, and then slightly decreases.

In contrast to the strong variation of μ_0 , T_m shows a slight increase from 17.7 K to 18.9 K, as P is increased from 0 to 1.3 GPa. A simple linear fit of T_m in this range yields a rate ~ 1.0 K/GPa, which roughly follows the reported P -variations of T_0 . Upon further compression, T_m jumps to 22 K at P_c , showing a spring of ~ 2.8 K from a value (~ 19.2 K) extrapolated with the above fit. For $P > P_c$, T_m again gradually increases and reaches ~ 23.5 K around 2.8 GPa. The pressure dependence of T_0 in this range is less clear, and the few available data points deviate from the behavior of T_m , see Fig. 6(b).

The lattice constant a , which is determined from the scans at (200), decreases slightly under pressure

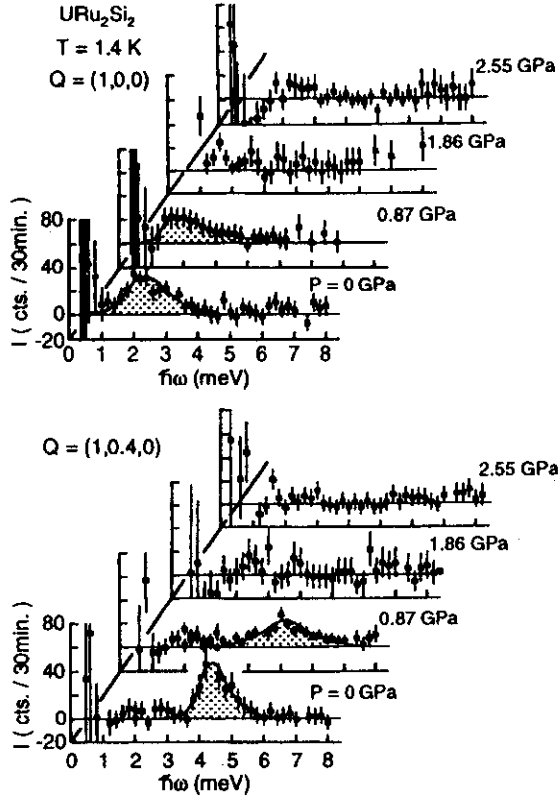


Fig. 7. Pressure variations of constant- Q scans at 1.4 K for $Q = (1, 0, 0)$ and $(1, 0, 4, 0)$ of URu₂Si₂. Incoherent scattering and the instrumental background are subtracted. The lines and shades are guides to the eye.

(Fig. 6(c)). From a linear fit of a at 1.4 K for $P < P_c$, we derive $-\partial \ln a / \partial P \sim 6.7 \times 10^{-4} \text{ GPa}^{-1}$. If the compression is isotropic, this yields an isothermal compressibility κ_T of $2 \times 10^{-3} \text{ GPa}^{-1}$, which is about 4 times smaller than what was previously estimated from the compressibilities of the constituent elements.⁴⁾

Around P_c , the lattice shrinks with a discontinuous change of $-\Delta a/a \sim 0.2\%$. Assuming again the isotropic compression, we evaluate $\Delta \ln V / \Delta \mu_0 \sim -0.04 \mu_B^{-1}$ and $\Delta \ln T_m / \Delta \ln V \sim -27$ associated with this transition. Note that a similar lattice anomaly at P_c is observed at 35 K, much higher than T_0 . This implies that the system has another energy scale characteristic of the volume shrinkage in the paramagnetic region.

To check the possibility of a structural phase transition at P_c , we have carefully investigated the widths of the nuclear reflections in longitudinal and radial scans at two equivalent reciprocal points of $(2, 0, 0)$ and $(0, 2, 0)$. No significant broadening of the peaks is detected at P_c , allowing us to conclude that there is no lattice distortion lowering the fourfold symmetry within the detectability limit of $|a - b|/a \sim 0.05\%$ and $\cos^{-1}(\hat{a} \cdot \hat{b}) \sim 2'$. The c axis is perpendicular to the scattering plane and cannot be measured in the present experimental configuration. Precise X-ray measurements under high pressure in an extended T -range are now in progress.

In Fig. 7, we plot the pressure variations of the energy scans at 1.4 K at $(1, 0, 0)$ and $(1, 0, 4, 0)$, after subtracting the instrumental background including incoherent scattering from the pressure cell and the sample. The background was measured by scans at the corresponding $|Q|$ -invariant positions $(0.702, 0.702, 0)$ and $(0.762, 0.762, 0)$, where the system is known to have neither magnon nor phonon excitations.⁵⁾ At ambient pressure, the observed spectra show clear peak anomalies centering around $\Delta_{(1,0,0)} \sim 2.3 \text{ meV}$ and $\Delta_{(1,0,0)} \sim 4.3 \text{ meV}$, which are in good agreement with the previous results.^{5,16)} For $P \sim 0.9 \text{ GPa}$, the peak intensity of the excitations is reduced by around half, but they still exist with roughly the same transfer energies. Above $P_c \sim 1.5 \text{ GPa}$, on the other hand, we could observe no significant anomalies at least within the energy range of $\hbar\omega \leq 8 \text{ meV}$. Large scattering amplitude at $\hbar\omega \sim 0$ for $(1, 0, 0)$ arises mainly from the magnetic Bragg scattering and the $\lambda/2$ nuclear reflections. For $(1, 0, 4, 0)$, on the other hand, it is mainly due to the statistical error in the subtraction.

§4. Discussion

4.1 A phenomenological analysis based on Landau's theory on the low-pressure ordered phase

The remarkable contrast between μ_0 and T_m below P_c offers a test to the various theoretical scenarios for the 17.5 K transition. Let us first examine the possibility of a single transition at $T_m (= T_0)$ due to magnetic dipoles. In general, Landau theory with a magnetic free energy

$$F_m = -a(T_m - T)m^2 + bm^4 - g\mu_B m h, \quad (1)$$

gives

$$m^2 = \frac{a}{2b}(T_m - T) \quad (2)$$

and

$$\Delta C/T_m \sim (Nk_B/T_m)(m_0/m_{\text{para}})^2, \quad (3)$$

where m and h denote the staggered dipole and field. Since T_m and ΔC are independent of g , their weak variations by pressure will be compatible with the ten-times enlargement of μ_0 ($\equiv g\mu_B m_0$), if only g is sensitive to pressure. The existing theories along this line explain the reduction of g by assuming crystalline-electric-field (CEF) effects with low-lying singlets,¹⁷⁾ and further by combining such with quantum spin fluctuations.^{18,19)} For small g -values, the theories predict the relations, $g \sim \exp(-\Delta/2k_B T_m)$ and $g \sim T_m/T^*$, where Δ and T^* denote the gap energy between two singlets and a characteristic energy of a quasi particle band. The observed behavior will thus be reproduced, if Δ and T^* is strongly reduced by applying pressure. Previous macroscopic studies however suggest opposite tendencies: the resistivity maximum at around 73 K ($P = 0$), which is usually regarded as T^* , shifts to higher temperatures^{35,37,39)} under pressure, and the low- T susceptibility, $\chi(0) \sim \Delta^{-1}$, decreases as P increases.³⁴⁾ The simple application of those models is thus unlikely to explain the behavior of μ_0 with pressure.

On the other hand, the models that predict a hidden order due to a non-dipolar degree of freedom ψ could be

consistent with the present observation. This category is further divided into two branches according to whether ψ is odd or even under time reversal, which we call (A) and (B) after the classification given by Shah *et al.*⁴⁵⁾ Three-spin order²¹⁾ and d-type spin density waves²⁷⁾ belong to the former, and quadrupolar order^{20, 22-24)} and structural distortions^{25, 26)} belong to the latter. We should notice that the polarized neutron scattering has confirmed that the reflections arise purely from magnetic dipoles.⁷⁾ For each branch, therefore, it has been proposed that the observed magnetic dipoles are induced by the order of ψ as secondary order.

The Landau free energy for type (A) theories is given as

$$F^{(A)} = -\alpha(T_0 - T)\psi^2 + \beta\psi^4 + Am^2 - \eta m\psi, \quad (4)$$

where α, β and A are positive, and the dimensionless order parameters m and ψ vary in the range $0 \leq m, \psi \leq 1$.⁴⁵⁾ Minimization of $F^{(A)}$ with respect to m gives $m = -\delta\psi$, where $\delta \equiv \eta/2A$, showing that the staggered dipole moment appears in proportion to the primary order parameter. The stability condition for ψ then yields a mean-field solution, $\psi^2 \sim \frac{\alpha}{2\beta}(T'_0 - T)$, where T'_0 denotes the renormalized transition temperature given as $T'_0 \sim T_0(1 + \kappa\delta^2)$. The coefficient κ is given as $A/\alpha T_0$, where A is originally written as $A = -a(T_m - T)$. Since $T_m \leq T_0$ and $\alpha \sim a \sim k_B$, κ is less than unity. Therefore, the shift of T_0 due to the coupling between ψ and m is the order of δ^2 . If the fluctuating dipole moment $\mu_{\text{para}} \sim 1.2 \mu_B$ seen above T_0 ¹⁶⁾ corresponds to the maximum induced value of the secondary order parameter ($m \sim 1$), then the observed increase in μ_0 gives the variation of δ ($\sim m_0 \sim \mu_0/\mu_{\text{para}}$) from 0.014 ($P = 0$) to 0.21 ($P \sim P_c$). This results in $dT_0/dP \sim T_0 dm_0^2/dP \sim 0.8$ K/GPa, which is in good agreement with the previous bulk measurements (~ 1.3 K/GPa).³⁴⁻³⁹⁾

In type (B), on the other hand, the simplest free energy invariant under time-reversal^{45, 46)} must take the form

$$F^{(B)} = -\alpha(T_0 - T)\psi^2 + \beta\psi^4 + a(T_m - T)m^2 + bm^4 - \zeta m^2\psi^2. \quad (5)$$

Minimization of $F^{(B)}$ with respect to ψ gives $\psi^2 = \frac{\alpha}{2\beta}(T'_0 - T)$, where $T'_0 = T_0 + \frac{\zeta}{\alpha}m^2$. Therefore, T_0 is unchanged, so far as m is continuously induced by the primary order ($m = 0$ at $T_m \leq T_0$). The secondary order of this type influences the specific heat at T_m as $\Delta C/T_m \sim Nk_B m_0^2/T_m$. By the same arguments as in type (A), we obtain $d(\Delta C/T_m)/dP \sim 20$ mJ/K²molGPa, when $T_m \sim T_0$. This cancels out with the P -increase in T_0 , resulting in a roughly P -independent jump in $C(T)$. This is consistent with previous $C(T)$ studies up to 0.6 GPa,³⁶⁾ in which $\Delta C_m/T_0$ is nearly constant, if entropy balance is considered. Note that in type (B) T_m can in principle differ from T_0 , which could also be consistent with the annealing effects.²⁸⁾

4.2 Quadrupolar and dipolar instabilities of the Γ_5 non-Kramers doublet

The phenomenological consideration shown above supports the hidden order hypotheses for the ordered phase

below P_c . We shall now argue more concretely that the staggered quadrupolar order due to the non-Kramers doublet Γ_5 fairly well explain the observed magnetic properties including the magnetic instability at P_c .

In our diluting experiments for $\text{Th}_{1-x}\text{U}_x\text{Ru}_2\text{Si}_2$ ($x \leq 0.07$), we have observed a strong uniaxial magnetic anisotropy with the c -axis susceptibility diverging down to ~ 0.1 K.²³⁾ This evidences a magnetically degenerate lowest state, and we have proposed the Γ_5 doublet to be the most promising CEF state to account for the observed anisotropy. The doublet is usually expressed as the form,

$$|\Gamma_5^\pm\rangle = \alpha|\pm 3\rangle + \beta|\mp 1\rangle, \quad (6)$$

where $|\pm \text{integer}\rangle$ denote the eigenfunctions for the z component of the total angular momentum of $J = 4$. $|\Gamma_5^\pm\rangle$ diagonalizes J_z with eigenvalues of $\pm(3\alpha^2 - \beta^2)$, but has no matrix elements for J_x and J_y . Therefore, Γ_5 always behaves as an Ising spin state for magnetic fields. Interestingly, Γ_5 may also behave as a quadrupolar doublet in response to strain fields of $\epsilon_{xx} - \epsilon_{yy}$ and ϵ_{xy} . One can see this by transforming the wave function (6) into

$$|\phi_1^\pm\rangle = \frac{1}{\sqrt{2}}(|\Gamma_5^+\rangle \pm |\Gamma_5^-\rangle) \quad (7)$$

and

$$|\phi_2^\pm\rangle = \frac{1}{\sqrt{2}}(|\Gamma_5^+\rangle \pm i|\Gamma_5^-\rangle), \quad (8)$$

which then diagonalize the quadrupolar operators $O_2^2 = J_x^2 - J_y^2$ and $P_{xy} = \frac{1}{2}(J_x J_y + J_y J_x)$ with eigenvalues of $\pm(6\sqrt{7}\alpha\beta + 10\beta^2)$ and $\pm(3\sqrt{7}\alpha\beta - 5\beta^2)$, respectively. Therefore, both the quadrupolar and dipolar orderings may occur in the system that has the Γ_5 lowest state. Note that these two instabilities compete with each other, since neither O_2^2 nor P_{xy} commutes with J_z . If the quadrupolar order takes place, then $|\phi_1^\pm\rangle$ or $|\phi_2^\pm\rangle$ splits into two quadrupolar singlets, shifting the dipolar matrix elements to off-diagonal. This is consistent with the feature of URu_2Si_2 that the phase transition at T_0 is accompanied by the diverging staggered susceptibility and the subsequent development of longitudinal magnon excitations.¹⁶⁾ The presence of the quadrupolar instability has also been suggested by recent measurements of elastic constants.⁴⁷⁾

The relationship between the quadrupolar and dipolar degrees of freedom in Γ_5 can be described in terms of a pseudo-spin $S = \frac{1}{2}$, if its components S_x, S_y and S_z are mapped onto O_2^2, P_{xy} and J_z , respectively. The quadrupolar order may occur when the spin-spin interactions are of XY -type. Ohkawa and Shimizu have recently pointed out this equivalence, and applied an extended s - d model to the Γ_5 local state. They have found that dynamical spin susceptibility along the c axis shows a peak anomaly in the vicinity of $\omega = 0$ and $Q = (1, 0, 0)$ as a result of the staggered quadrupolar order.²⁴⁾ From the calculations they attribute the tiny dipole moments to the dynamical spin fluctuations with a life time in between the time scales of static and neutron scattering measurements. This is supported by recent NMR measurements under pressure, in which the dipolar order has not been observed even for $P \sim 0.4$ GPa.⁵¹⁾

Interestingly, they have further proposed the phase transition at P_c to be a switching in the order parameter between quadrupole and dipole in Γ_5 . Opposite to the above situation, the dipolar order splits $|\Gamma_5^\pm\rangle$ into two singlets, which are coupled with each other only by O_2^2 or P_{xy} . Therefore, the magnon excitations should disappear in the dipolar ordered state of Γ_5 . This is consistent with the present results of inelastic neutron scattering, at least, in the survey ranging up to 8 meV (Fig. 7). Note that electrical resistivity below T_0 follows a gap-type function even for $P > P_c$,^{37,39)} evidencing the presence of excitations that can be detected by thermal probes.

§5. Conclusion

We have found URu₂Si₂ to undergo a new phase transition under high pressure, at $P_c \sim 1.5$ GPa. Below P_c , the sublattice magnetization associated with the 17.5 K transition is strongly enhanced, where the unusual T -linear behavior is conserved. In contrast to the ten-times increase in the saturation moment, however, the transition temperature rises only ten percent with pressure. These results for $P < P_c$ could indicate that the tiny dipole moments are intrinsically induced by the 17.5 K transition, but that they are not the primary order parameter. A simple analysis based on the Landau's theory supports the hidden (non-dipolar) order scenarios. Above P_c , on the other hand, the T variations of the staggered moment are well described by a 3D-Ising model, where sharp magnon excitations below P_c disappear. We have shown that the magnetic instabilities at P_c as well as the exotic phase below P_c could be ascribed to the competitions between the quadrupolar and dipolar degrees of freedom in the Γ_5 non-Kramers doublet. In this context the low-pressure phase will be described as a staggered quadrupolar ordered state concomitant with dynamical spin fluctuations.²⁴⁾ To obtain a conclusive proof, we are making the resonant X-ray scattering and the NMR measurements in a wide P -range.

Acknowledgements

One of us (H.A.) is indebted to F.J. Ohkawa for helpful discussions. This work was partly supported by the JAERI-JRR3M Collaborative Research Program, and by Grant-in-Aid for Scientific Research from Ministry of Education, Science, Sports and Culture of Japan.

- 1) T.T.M. Palstra, A.A. Menovsky, J. van den Berg, A.J. Dirkmaat, P.H. Kes, G.J. Nieuwenhuys and J.A. Mydosh: Phys. Rev. Lett. **55**(1985)2727.
- 2) W. Schlitz, J. Baumann, B. Pollit, U. Rauchschwalbe, H.M. Mayer, U. Ahlheim and C.D. Bredl: Z. Phys. **B62**(1986)171.
- 3) M.B. Maple, J.W. Chen, Y. Dalichaouch, T. Kohara, C. Rossel, M.S. Torikachvili, M.W. McElfresh and J.D. Thompson: Phys. Rev. Lett. **56**(1986)185.
- 4) A. de Visser et al., F.E. Kayzel, A.A. Menovsky, J.J.M. Franse, J. van den Berg and G.J. Nieuwenhuys: Phys. Rev. **B34**(1986)8168.
- 5) C. Broholm, J.K. Kjems, W.J.L. Buyers, P. Matthews T.T.M. Palstra, A.A. Menovsky and J.A. Mydosh: Phys. Rev. Lett. **58**(1987)1467; C. Broholm, H. Lin, P.T. Matthews, T.E. Mason, W.J.L. Buyers, M.F. Collins, A.A. Menovsky, J.A. Mydosh and J.K. Kjems: Phys. Rev. **B43**(1991)12809.
- 6) T.E. Mason, B.D. Gaulin, J.D. Garrett, Z. Tun, W.J.L. Buyers and E.D. Isaacs: Phys. Rev. Lett. **65**(1990)3189.
- 7) M.B. Walker, W.J.L. Buyers, Z. Tun, W. Que, A.A. Menovsky and J.D. Garrett: Phys. Rev. Lett. **71**(1993)2630.
- 8) E.D. Isaacs, D.B. McWhan, R.N. Kleiman, D.J. Bishop, G.E. Ice, P. Zschack, B.D. Gaulin, T.E. Mason, J.D. Garrett and W.J.L. Buyers: Phys. Rev. Lett. **65**(1990)3185.
- 9) G. Aeppli, E. Bucher, C. Broholm, J.K. Kjems, J. Baumann and J. Hufnagl: Phys. Rev. Lett. **60**(1988)615.
- 10) S. Kawarazaki: submitted to the Workshop on "Frontiers in Magnetism", October 4-7, 1999, Kyoto; to be published in J. Phys. Soc. Jpn.
- 11) See, for example, a discussion given by W.J.L. Buyers: Physica **B223&224**(1996)9.
- 12) T.T.M. Palstra, A.A. Menovsky and J.A. Mydosh: Phys. Rev. **B33**(1986)6527.
- 13) U. Walter, C.-K. Loong, M. Loewnhaupt and W. Schlitz: Phys. Rev. **B33**(1986)7875.
- 14) D.A. Bonn, J.D. Garrett and T. Timusk: Phys. Rev. Lett. **61**(1988)1305.
- 15) J. Aarts, A.P. Volodin, A.A. Menovsky, G.J. Nieuwenhuys and J.A. Mydosh: Europhys. Lett. **26**(1994)203.
- 16) T.E. Mason, W.J.L. Buyers, T. Peterson, A.A. Menovsky and J.D. Garrett: J. Phys.: Condens. Matter **7**(1995)5089.
- 17) G.J. Nieuwenhuys: Phys. Rev. **B35**(1987)5260.
- 18) A.E. Sikkema, W.J.L. Buyers, I. Affleck and J. Gan: Phys. Rev. **B54**(1996)9322.
- 19) Y. Okuno and K. Miyake: J. Phys. Soc. Jpn. **67**(1998)2469.
- 20) Y. Miyako, S. Kawarazaki, H. Amitsuka, C.C. Paulsen and K. Hasselbach: J. Appl. Phys. **76**(1991)5791.
- 21) V. Barzykin and L.P. Gor'kov: Phys. Rev. Lett. **70**(1993)2479.
- 22) P. Santini and G. Amoretti: Phys. Rev. Lett. **73**(1994)1027; **74**(1995)4098; P. Santini: Phys. Rev. **B57**(1998)5191.
- 23) H. Amitsuka and T. Sakakibara: J. Phys. Soc. Jpn. **63**(1994)736.
- 24) F.J. Ohkawa and H. Shimizu: J. Phys.: Condens. Matter **11**(1999)L519.
- 25) V. Barzykin and L.P. Gor'kov: Phys. Rev. Lett. **74**(1995)3723.
- 26) T. Kasuya: J. Phys. Soc. Jpn. **66**(1997)3348.
- 27) H. Ikeda and Y. Ohashi: Phys. Rev. Lett. **81**(1998)3723.
- 28) B. Fåk, C. Vettier, J. Flouquet, F. Bourdarot, S. Raymond, A. Vernière, P. Lejay, Ph. Bouteauille, N.R. Bernhoeft, S.T. Bramwell, R.A. Fisher and N.E. Phillips: J. Magn. Magn. Mater. **154**(1996)339.
- 29) S.A.M. Mentink, T.E. Mason, S. Süllo, G.J. Nieuwenhuys, A.A. Menovsky, J.A. Mydosh and J.A.A.J. Perenboom: Phys. Rev. **B53**(1996)R6014.
- 30) N.H. van Dijk, F. Bourdarot, J.C.P. Klaasse, I.H. Hagmusa, E. Brück and A.A. Menovsky: Phys. Rev. **B56**(1997)14493.
- 31) S.A.M. Mentink, U. Wyder, J.A.A.J. Perenboom, A. de Visser, A.A. Menovsky, G.J. Nieuwenhuys, J.A. Mydosh and T.E. Mason: Physica **B230-232**(1997)74.
- 32) T. Kohara, Y. Kohori, K. Asayama, Y. Kitaoka, M.B. Maple and M.S. Torikachvili: Solid State Commun. **59**(1986)603.
- 33) O.O. Bernal, B. Becker, J.A. Mydosh, G.J. Nieuwenhuys, A.A. Menovsky, P.M. Paulus, H.B. Brom, D.E. MacLaughlin and H.G. Lukefahr: to be published in Physica B.
- 34) E. Louis, A. de Visser, A.A. Menovsky, J.J.M. Franse: Physica **144B**(1986)48.
- 35) M.W. McElfresh, J.D. Thompson, J.O. Willis, M.B. Maple, T. Kohara and M.S. Torikachvili: Phys. Rev. **B35**(1987)43.
- 36) R.A. Fisher, S. Kim, Y. Wu, N.E. Phillips, M.W. McElfresh, M.S. Torikachvili and M.B. Maple: Physica **B163**(1990)419.
- 37) M. Ido, Y. Segawa, H. Amitsuka and Y. Miyako: J. Phys. Soc. Jpn. **62**(1993)2962.
- 38) L. Schmidt: Ph.D. thesis, Joseph Fourier University (Grenoble), 1993 (unpublished).
- 39) G. Oomi, T. Kagayama, Y. Ōnuki and T. Komatsubara: Physica **B199&200**(1994)148.
- 40) H. Amitsuka, M. Sato, N. Metoki, M. Yokoyama, K.

- Kuwahara, T. Sakakibara, H. Morimoto, S. Kawarazaki, Y. Miyako, and J.A. Mydosh: *Phys. Rev. Lett.* **83**(1999)5114.
- 41) A. Onodera, Y. Nakai, N. Kunimori, O.A. Pringle, H.G. Smith, R.M. Nicklow, R.M. Moon, F. Amita, N. Yamamoto, S. Kawano, N. Achiwa and Y. Endoh: *Jpn. J. Appl. Phys.* **26**(1987)152.
- 42) B.C. Frazer, G. Shirane, D.E. Cox and C.E. Olsen: *Phys. Rev.* **140**(1965)A1448.
- 43) D.M. Burley: *Phil. Mag.* **5**(1960)909.
- 44) R. Kubo: *Phys. Rev.* **87**(1952)568.
- 45) N. Shah, P. Chandra, P. Coleman and J.A. Mydosh: (to be published in *Phys. Rev. B*).
- 46) M.B. Walker and W.J.L. Buyers: *Comment, Phys. Rev. Lett.* **74**(1995)4097.
- 47) K. Kuwahara, H. Amitsuka, T. Sakakibara, O. Suzuki, S. Nakamura, T. Goto, M. Mihalik, A.A. Menovsky, A. de Visser and J.J.M. Franse: *J. Phys. Soc. Jpn.* **66**(1997)3251; K. Kuwahara, A. Okumura, M. Yokoyama, K. Tenya, H. Amitsuka and T. Sakakibara: to be published in *Physica B*.
- 48) T. Honma, Y. Haga, E. Yamamoto, N. Metoki, Y. Koike, H. Ohkuni, N. Suzuki and Y. Ōnuki: *J. Phys. Soc. Jpn.* **68**(1999)338.
- 49) D.E. MacLaughlin, D.W. Cooke, R.H. Heffner, R.L. Hutson, M.W. McElfresh, M.E. Schillaci, H.D. Rempp, J.L. Smith, J.O. Willis, E. Zirngiebl, C. Boekema, R.L. Lichti and J. Oostens: *Phys. Rev. B* **37**(1988)3153.
- 50) L. Onsager: *Phys. Rev.* **65**(1944)117.
- 51) K. Matsuda, Y. Kohori and T. Kohara: private communication.

Hidden Order in URu_2Si_2 Studied by High-Pressure Experiments

Hokkaido University , Sapporo, JAPAN
Hiroshi Amitsuka

Backgrounds

5f Systems

The “17.5K Transition” of URu_2Si_2

Neutron Scat. Exper. under High-P

Ohkawa Model

Advances and Prospects

Collaborators

M. Yokoyama, K. Tenya, T. Sakakibara, F.J. Ohkawa
Graduate School of Science, Hokkaido University

M. Sato, N. Metoki
Advanced Science Research Center, JAERI

K. Kuwahara
Graduate School of Science, Tokyo Metropolitan University

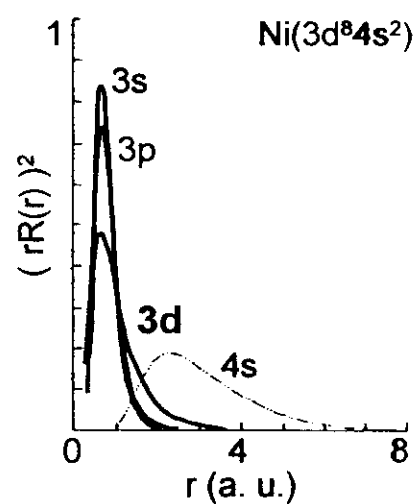
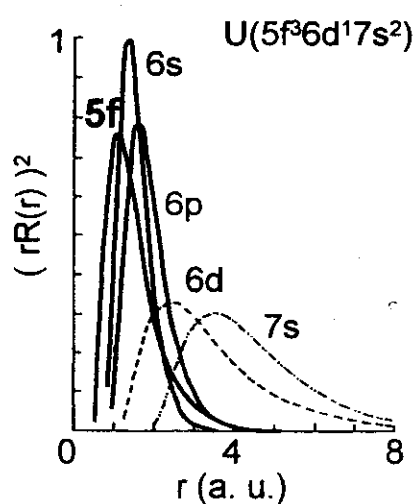
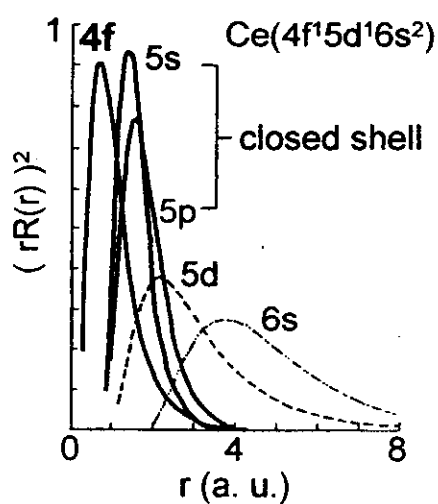
S. Kawarazaki, Y. Miyako
Graduate School of Science, Osaka University

S. Ramakrishnan
Tata Institute of Fundamental Research, Bombay, India

J.A. Mydosh
Kamarlingh Onnes Laboratory, Leiden Univ. The Netherlands

5f States

Ionic : $\langle r \rangle_{4f} < \langle r \rangle_{5f} < \langle r \rangle_{3d}$



Periodic



4f

Intra-Atomic
Many-Body States
+
c-f Hybridization

5f

?

3d

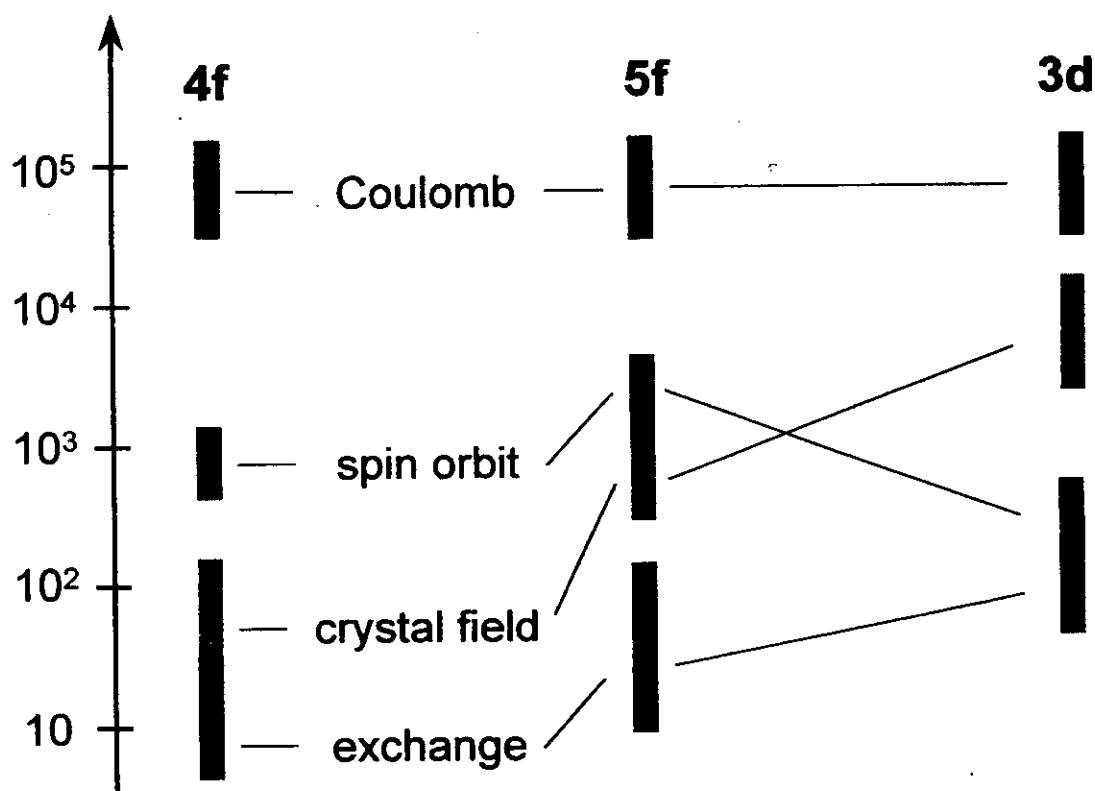
Bands
+
Spin Fluctuations

T. Kasuya JPSJ (Japanese ed.)42(1987)722

5f States

Standard Energy Scale

Energy (K)



Handbook on the Physics and Chemistry of the Actinides,
 edited by A.J. Freeman and G.H. Lander,
 Elsevier Sci. Pub., Chapter 2, 1985, p. 34

Topics in the Strongly Correlated 5f Electron Systems

Unconventional Superconductivity

UPt_3 , UPd_2Al_3 , URu_2Si_2 , UBe_{13}

Tiny or Small Moment Magnetism

UPt_3 , URu_2Si_2 ,	\rightarrow	$\mu_{\text{ord}} \sim 10^{-2} \mu_B$
UPd_2Al_3 , UNi_2Al_3 , UIr_2Si_2	\rightarrow	$\sim 10^{-1} \mu_B$

Non-Dipolar Order?

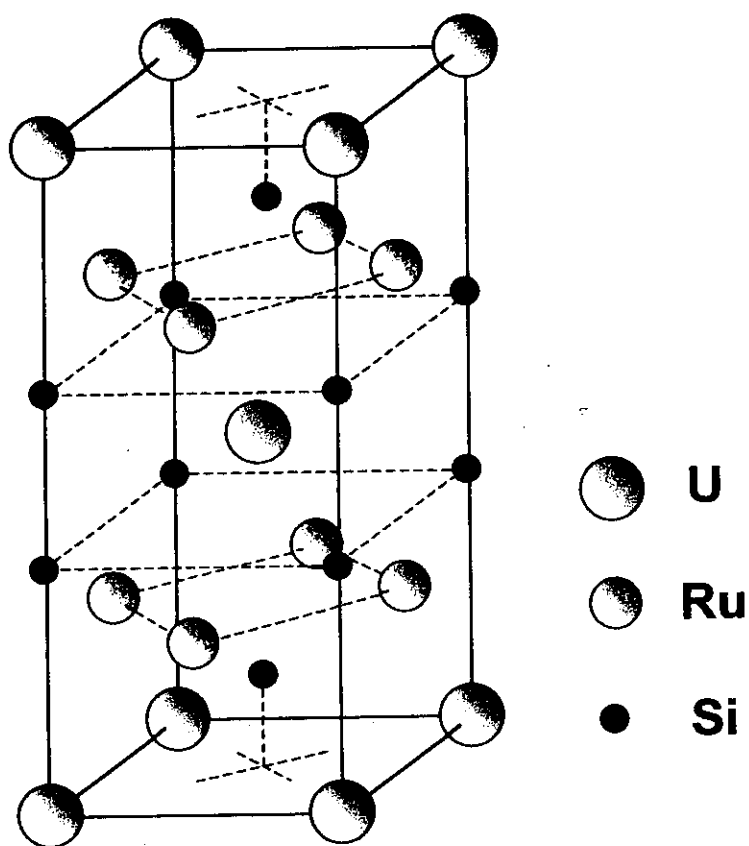
UPd_3 , URu_2Si_2 , UCu_2Sn

Quadrupoles ?

Quadrupolar Kondo Effects and NFL?

$(\underline{\text{Y}}, \text{U})\text{Pd}_3$, $(\underline{\text{Th}}, \text{U})\text{Be}_{13}$,
 $(\underline{\text{Th}}, \text{U})\text{Ru}_2\text{Si}_2$

an Exotic
Local c-f Interaction ?



ThCr₂Si₂ structure (I4/mmm)

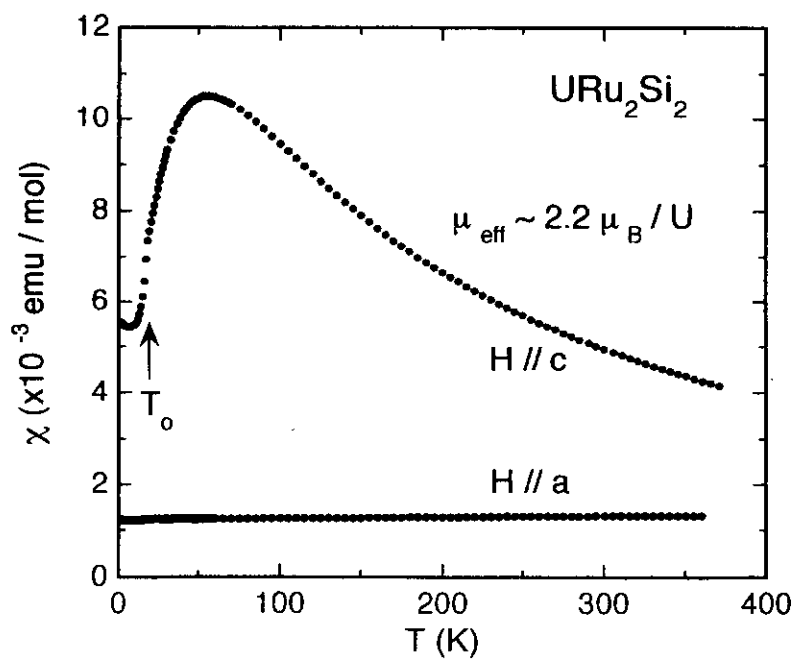
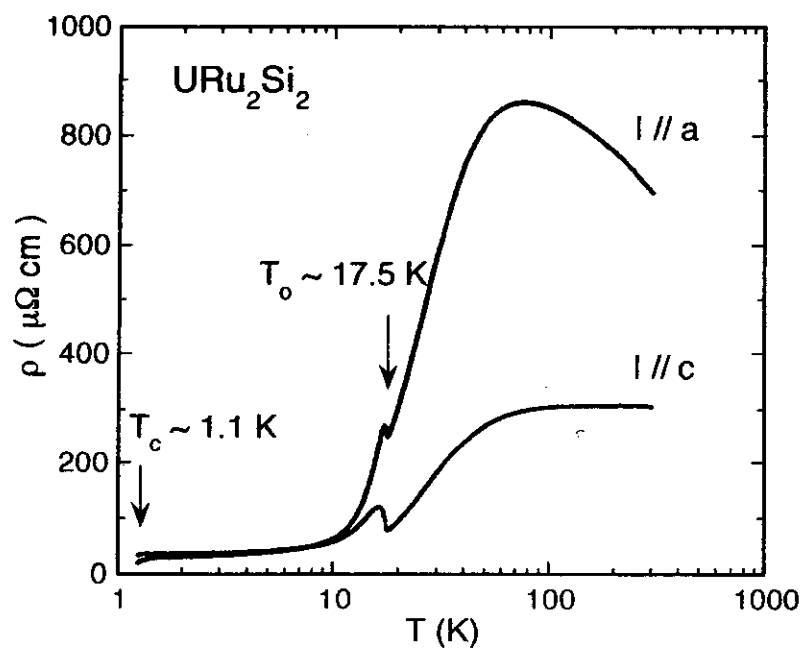
	a (Å)	c (Å)	V (Å ³)
URu ₂ Si ₂	4.127	9.570	163

ρ & χ

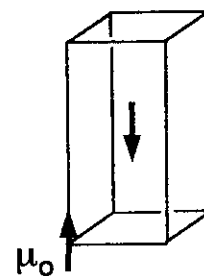
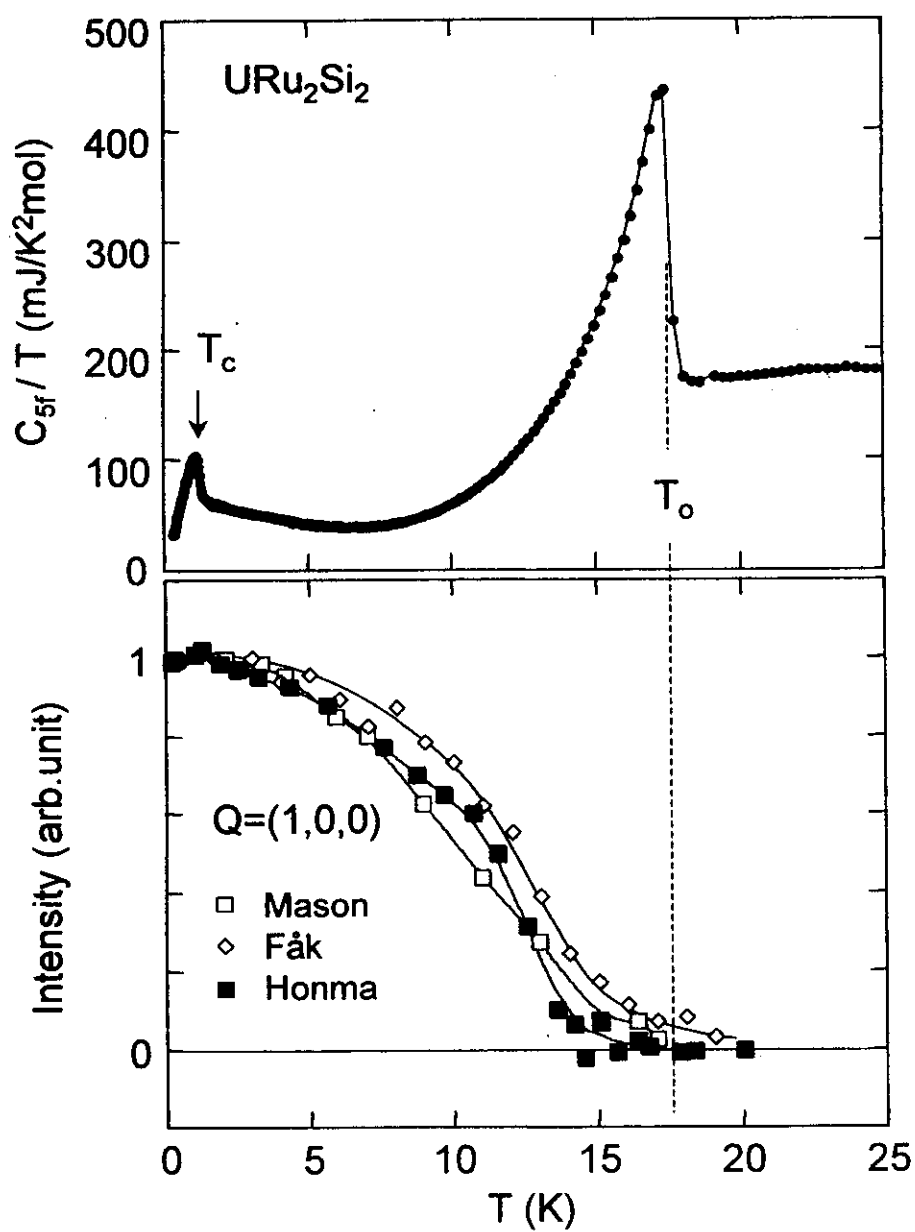
T.T.M. Palstra et al., PRL55(1985)2727

W. Schlitz et al., Z. Phys. B62(1986)171

M.B. Maple et al., PRL56(1986)185



C/T & Tiny-Moment AF State

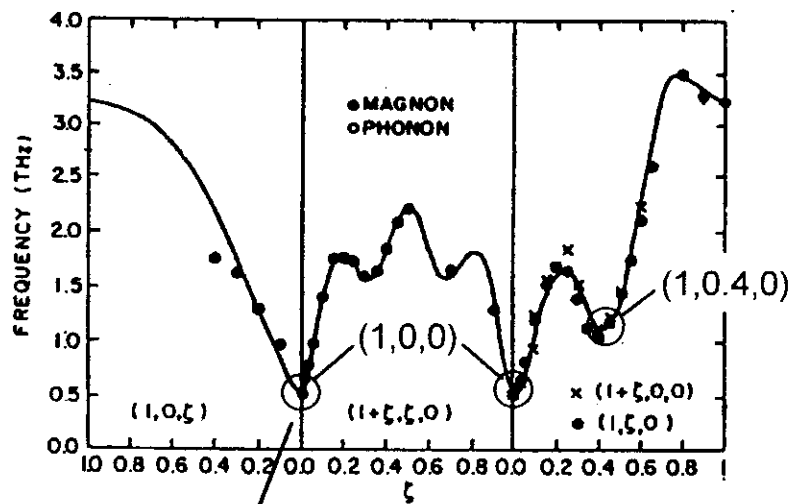


$$\mu_o \sim 0.02 - 0.04 \mu_B$$

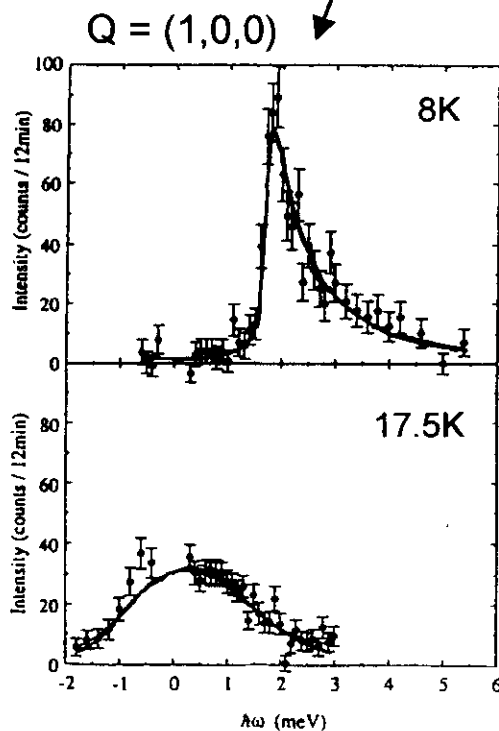
$$\xi_c \sim 100 \text{ \AA}$$

$$\xi_a \sim 300 \text{ \AA}$$

Magnon excitations



C. Broholm et al.
PRB43(1991)12809

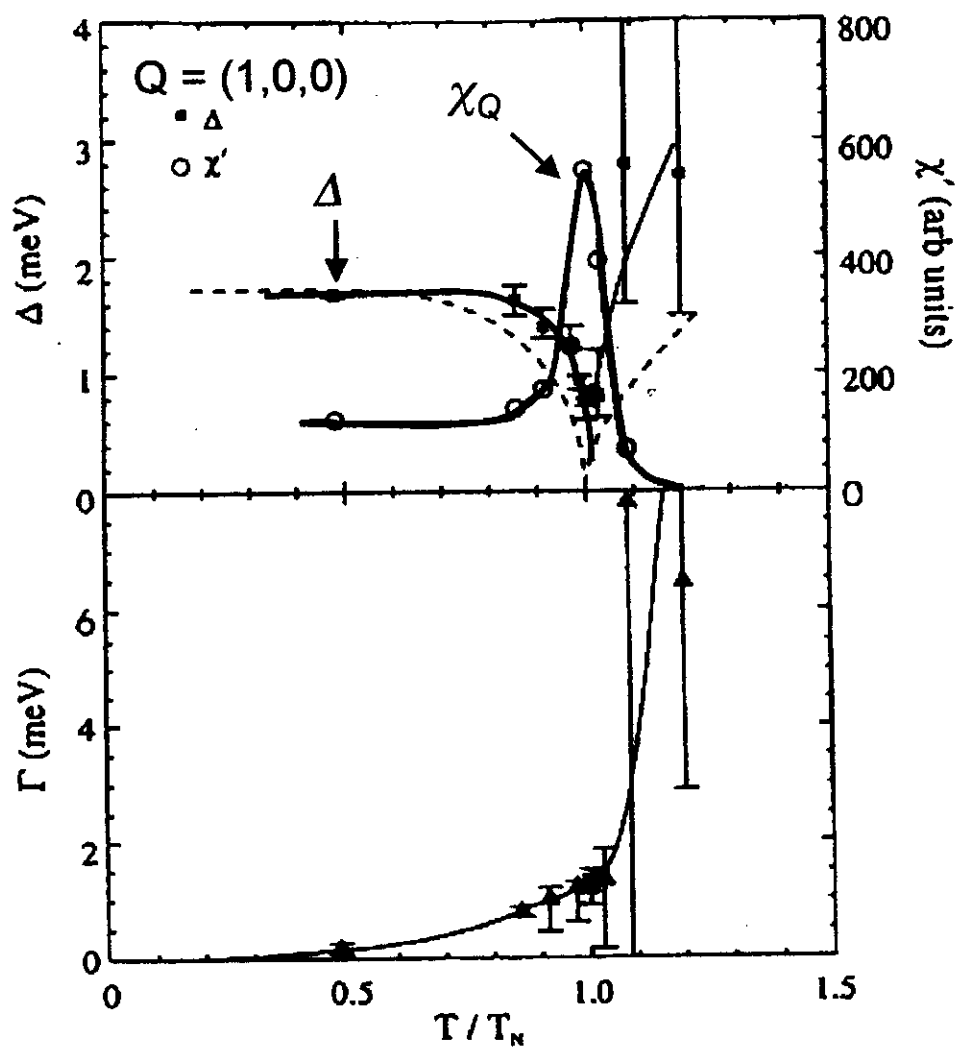


$$\chi_q^{zz} \propto \frac{2\Delta g^2 \mu_B^2 |\langle 0 | S^z | 1 \rangle|^2}{\omega_q^2 - \omega^2}$$

$$g\mu_B |\langle 0 | S^z | 1 \rangle| \sim 1.2 \mu_B$$

T.E. Mason et al.
J. Phys. 7(1995)5089

χ_Q



T.E. Mason et al.
J. Phys. 7(1995)5089

If f electrons are well localized

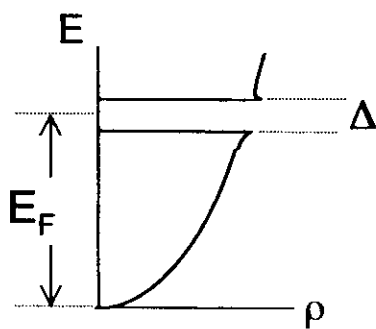
$$\frac{\Delta C}{T_N} \sim \frac{Nk_B}{T_N} \left[\frac{\mu_o}{\mu_{para}} \right]^2$$

$$\left\{ \begin{array}{l} \mu_o \sim 0.03 \mu_B \\ \mu_{para} \sim 1.2 \mu_B \end{array} \right.$$

$$\sim 0.3 \text{ mJ/K}^2\text{mol}$$

by experiments ... \updownarrow 300 mJ/K²mol

If they are itinerant



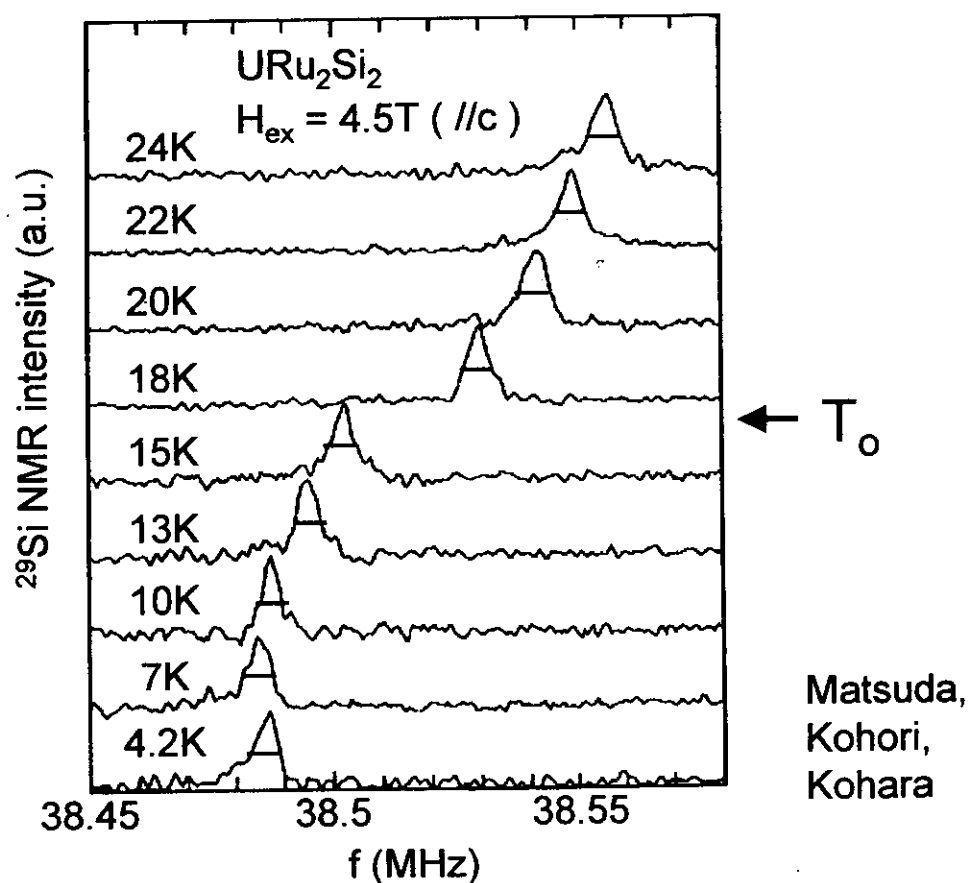
$$\mu_o \sim \mu_B \times \left[\frac{\Delta}{E_F} \right] \sim 0.03 \mu_B$$

$$S_{mag} \sim R \ln 2 \times \left[\frac{\Delta}{E_F} \right] \sim 0.03 R \ln 2$$

by experiments ... \updownarrow $\sim 0.2 R \ln 2$

^{29}Si NMR

Absence of internal fields below T_0 .



Are the tiny moments quasi-static fluctuations?



$$10^{-5} < \tau(\text{s}) < 10^{-10}$$

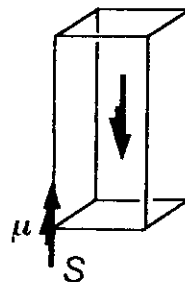
Proposed Scenarios for the Order Parameter

Magnetic Dipoles ?

Small g-factor

Crystal Fields?

Quantum Spin Fluctuations



*Niewenhuys '88
Sikkema '96
Okuno, Miyake '98
Yamagami '99*

Intrinsic (static)

Hidden OP ?

Quadrupole

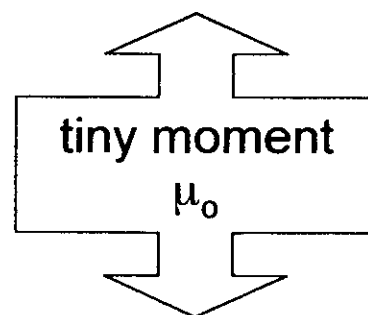
*Miyako '91
Santini, Amoretti '94
Amitsuka '94
Ohkawa '99
Tsuruta '00*

U-pair

Kasuya '97

d-wave SDW *Ikebe, Ohashi '98*

Valece+Str. *Barzykin, Gorkov*

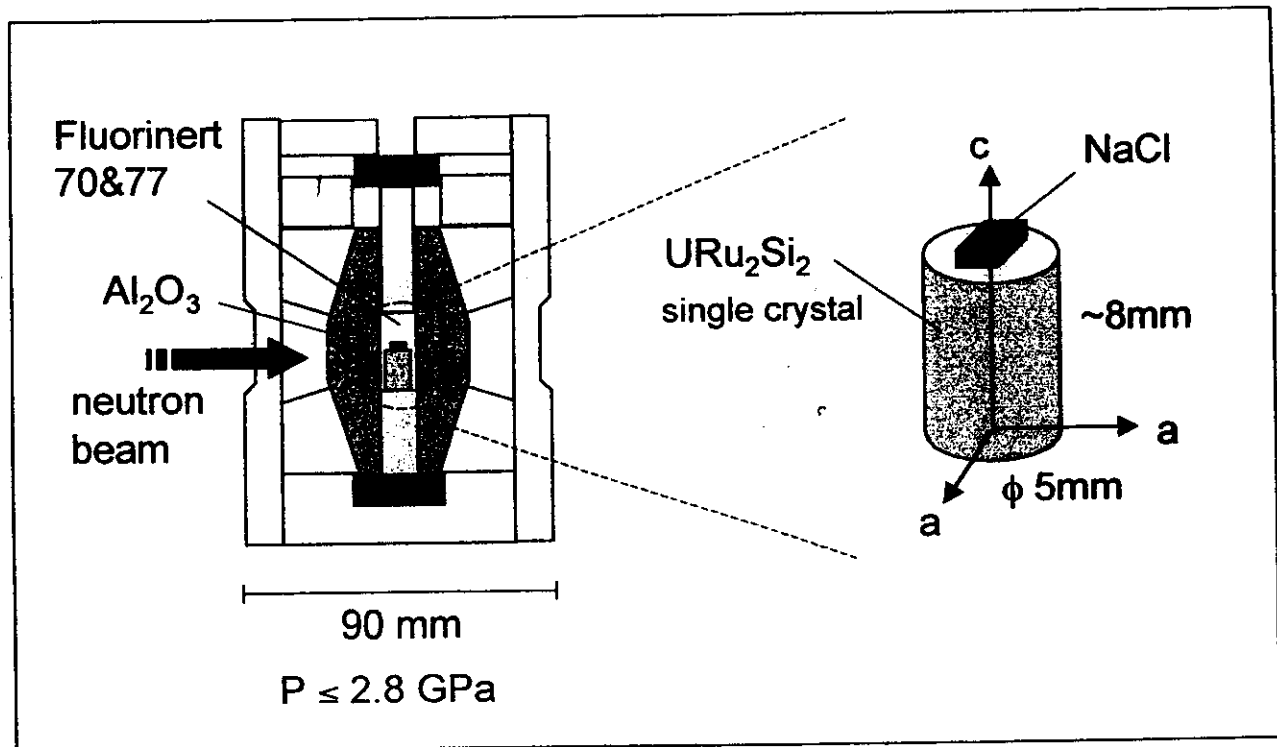


Side effects

fluctuations?

a parasitic phase?

Neutron Scattering Experiments under High Pressure

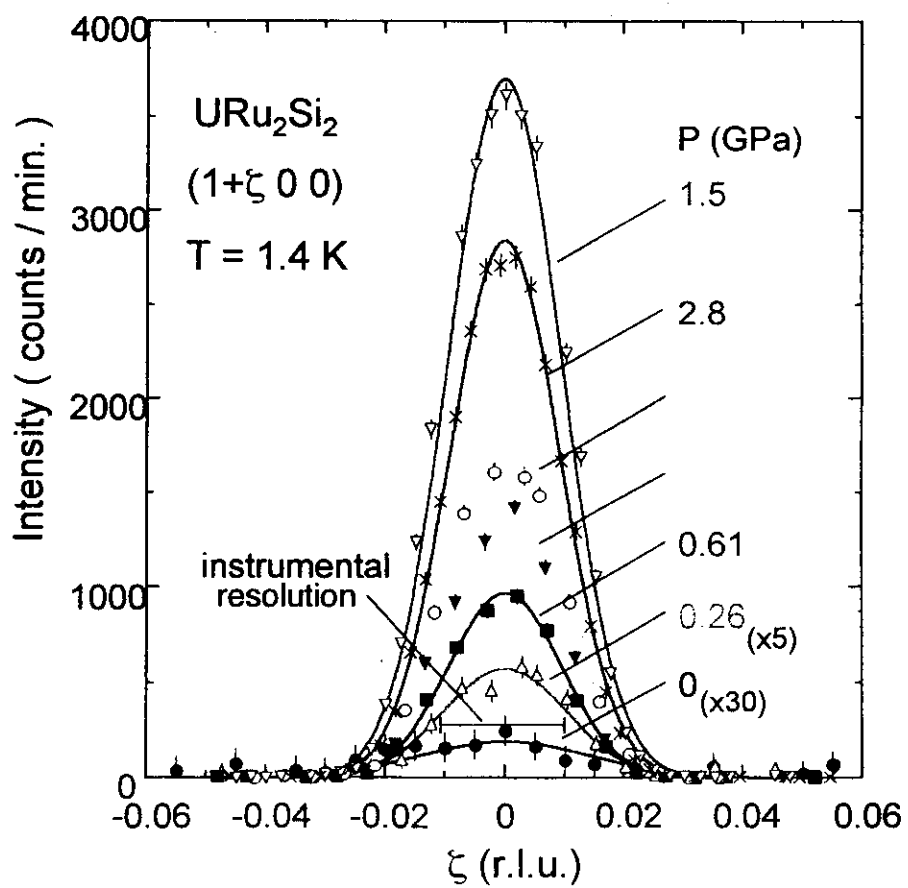
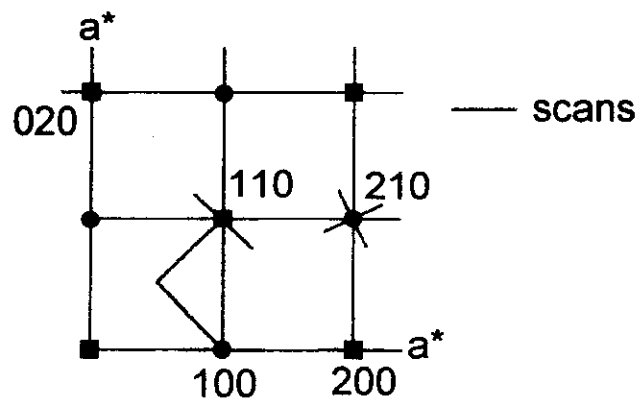


TAS-1 (JRR-3M, JAERI)

Elastic: $k_i = k_f = 2.6679 \text{ \AA}^{-1}$
 $40' - 80' - 40' - 80'$ (Al_2O_3 & PG $\times 2$ filters)

Inelastic: $k_i = 2.6635 \text{ \AA}^{-1}$ fixed
 $B - 80' - 40' - 80'$ (Al_2O_3 & PG $\times 1$ filters)

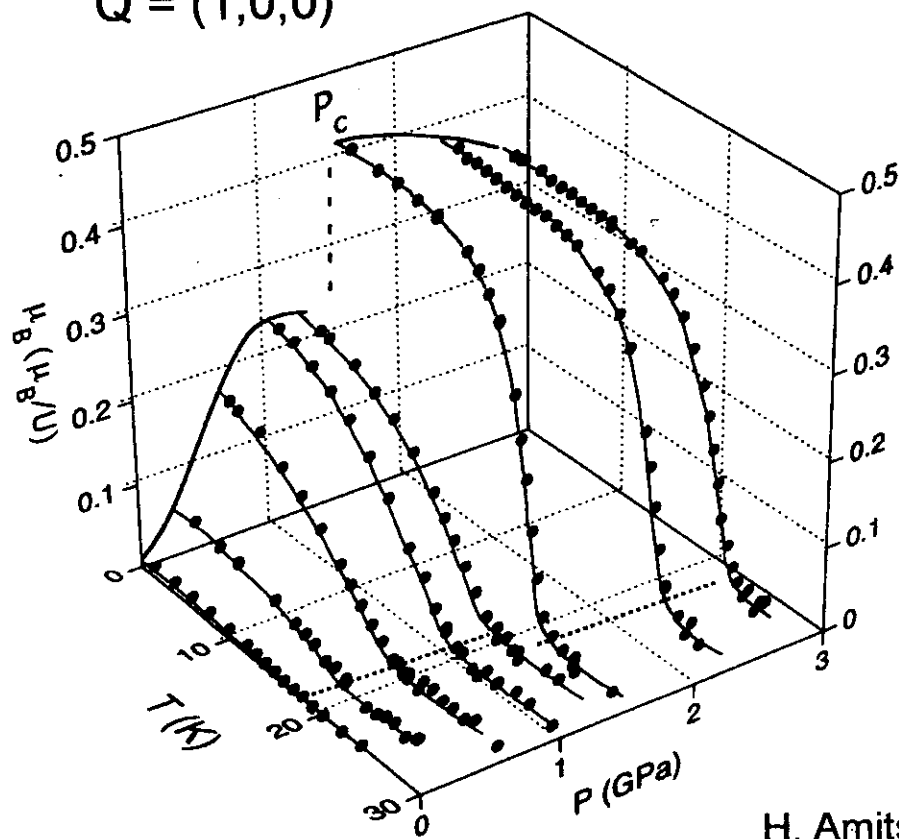
Elastic scattering



$$\mu_o(P, T)$$

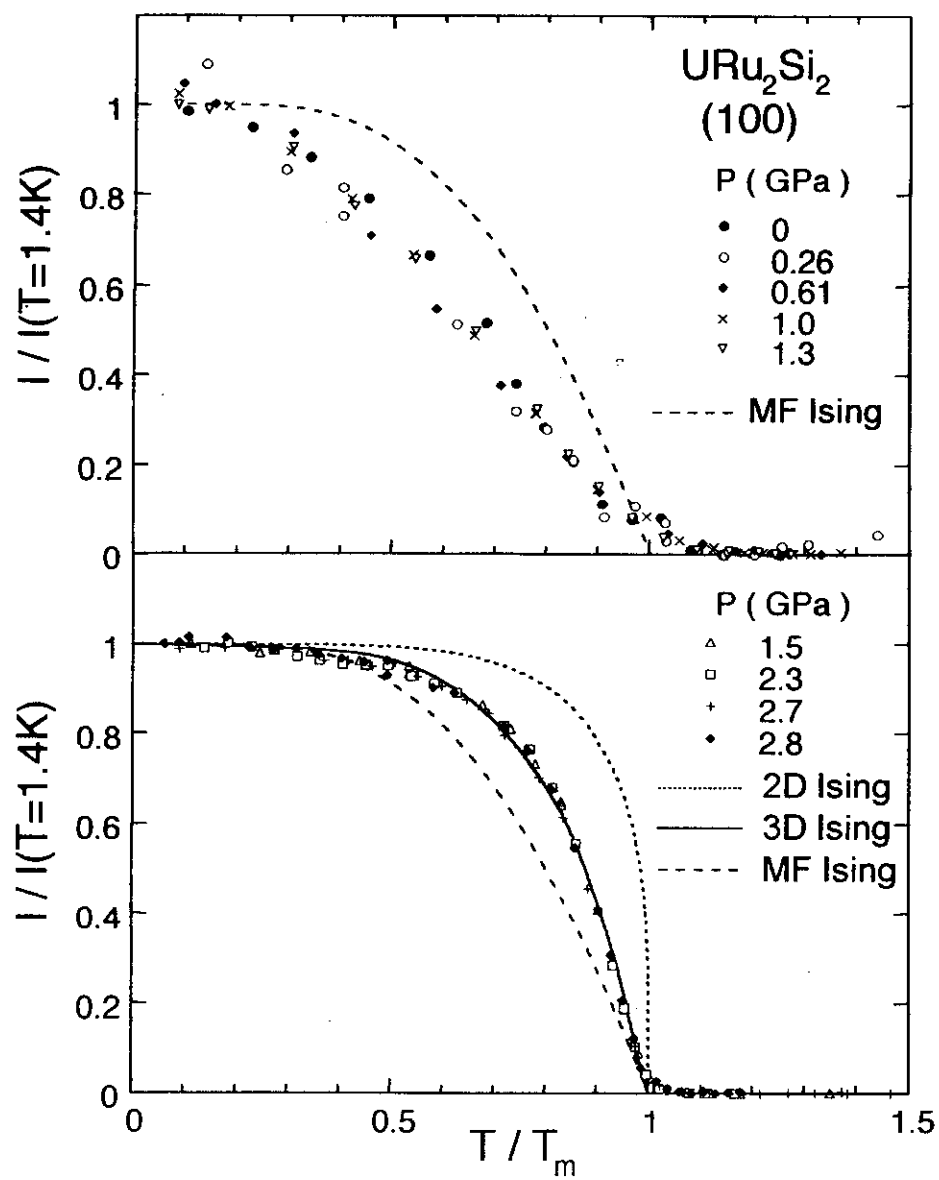
URu₂Si₂
Q = (1,0,0)

$k_i = 2.6679 \text{ \AA}^{-1}$
TAS-1: 40'-80'-40'-80'

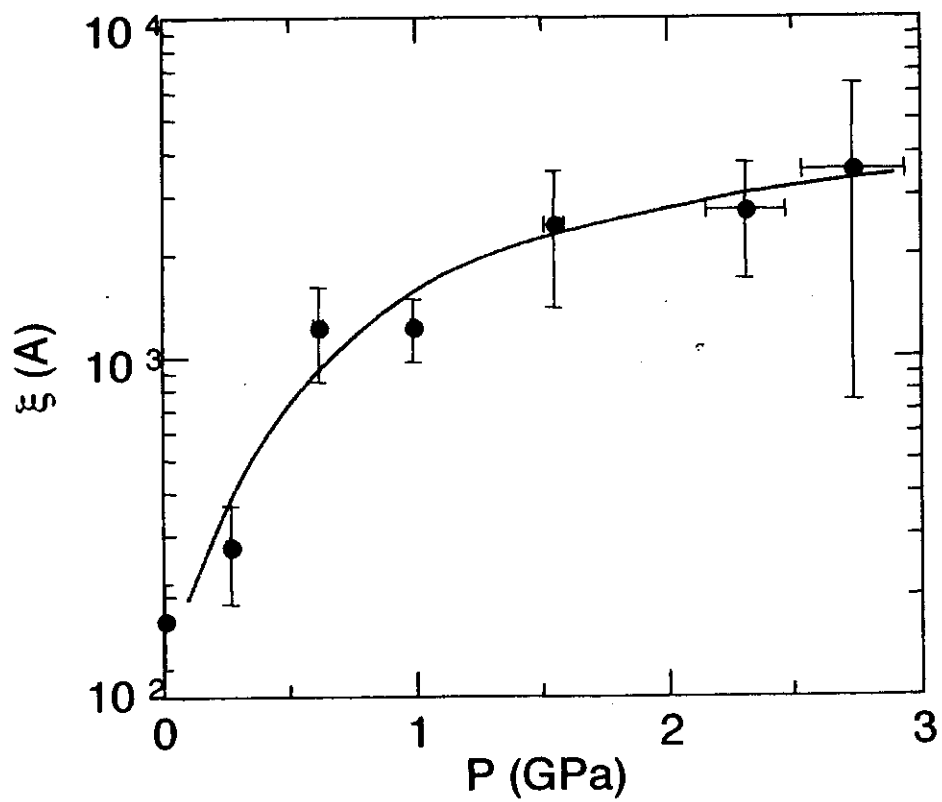


H. Amitsuka et al.
PRL 83(1999)5114

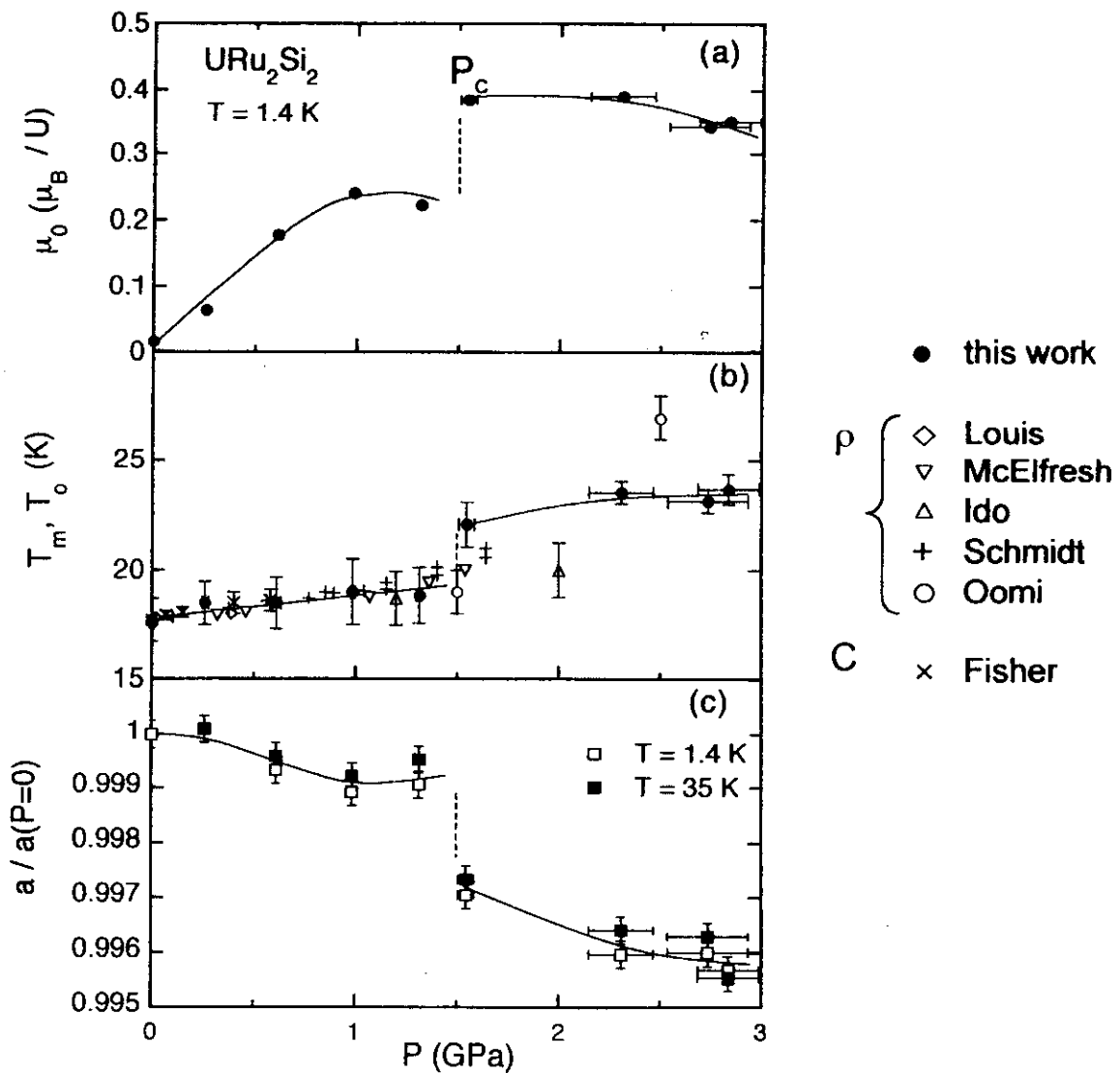
I / I_0 vs T / T_m



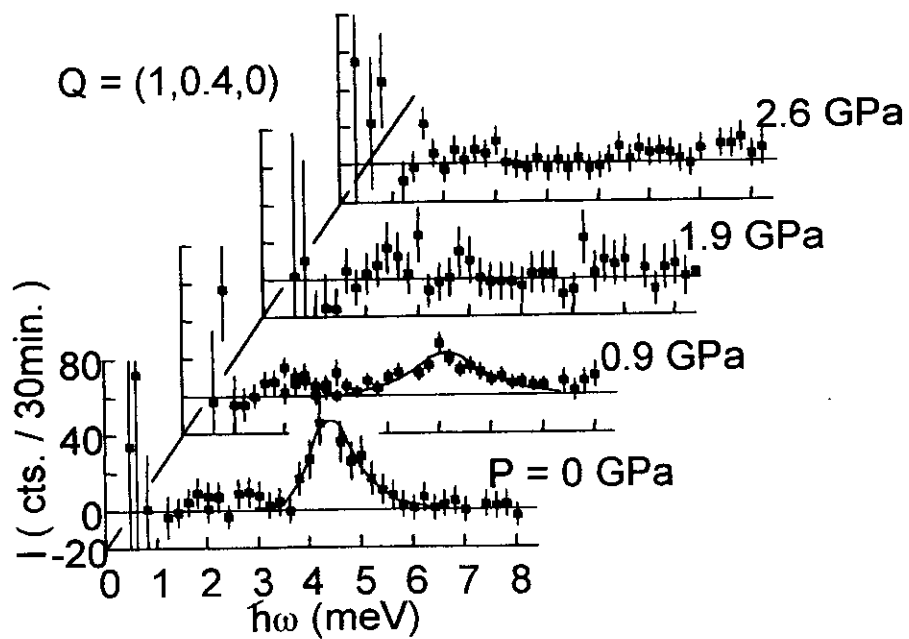
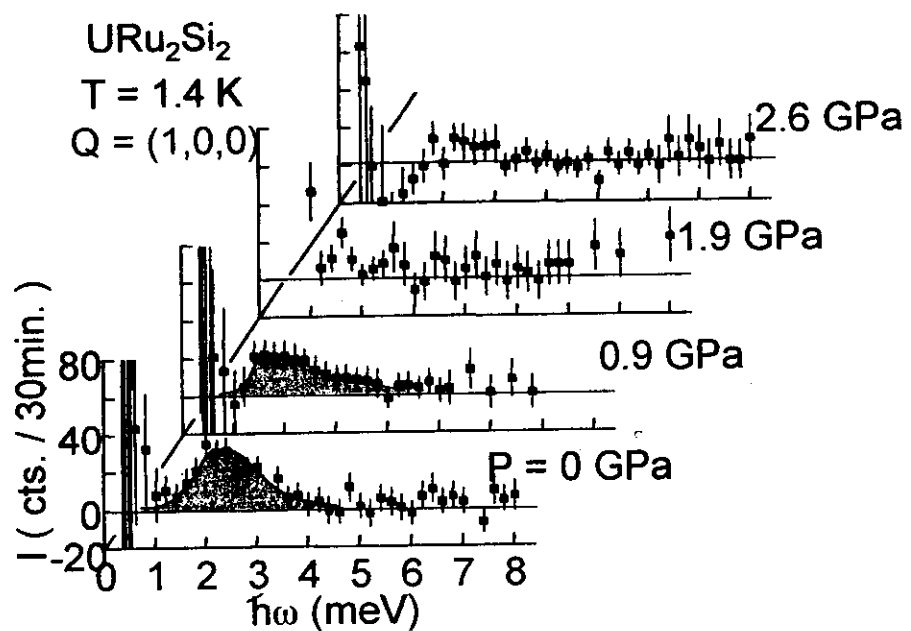
Coherence length



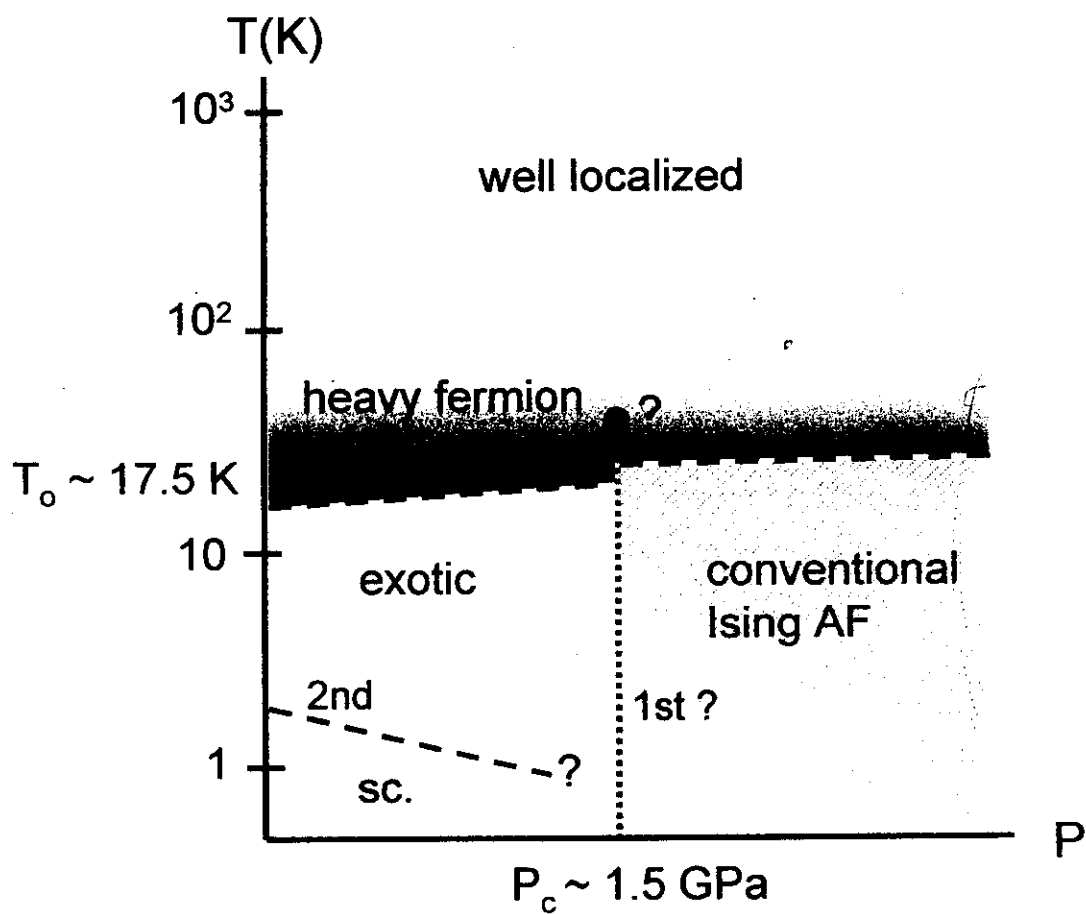
P variations of μ_0 , T_m , T_o , and the lattice parameter a



Inelastic scattering

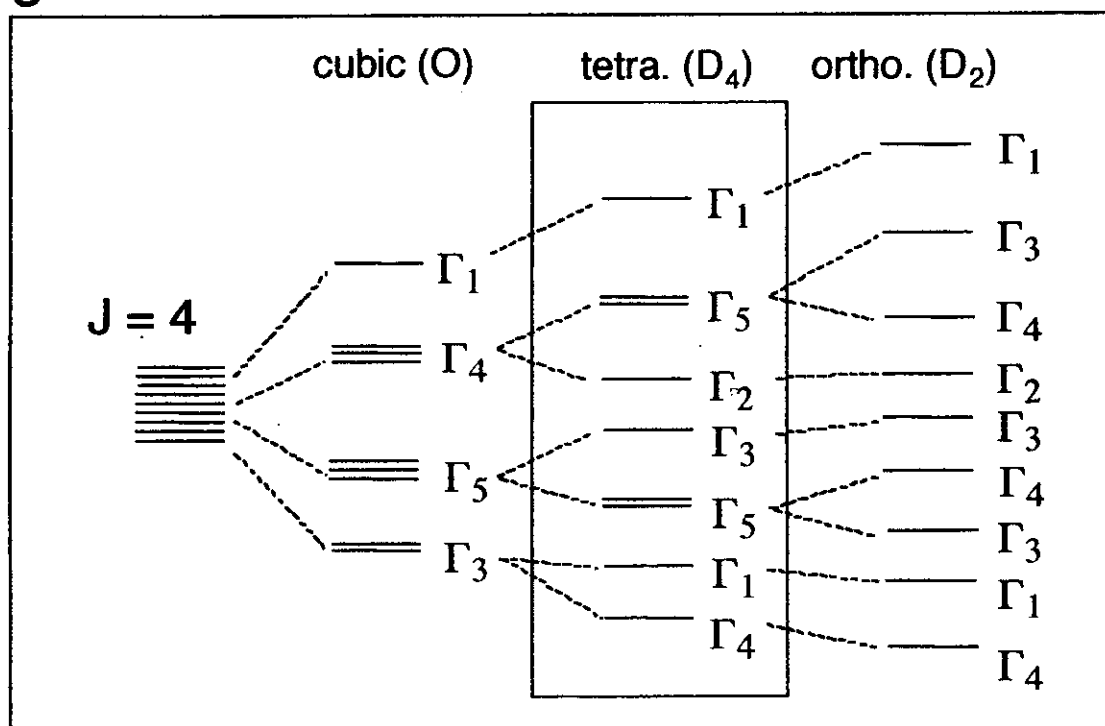


P-T phase diagram



CEF branching in $f^2(U^{4+})$ configuration

In general....



Is the CEF lowest state of URu_2Si_2 ...

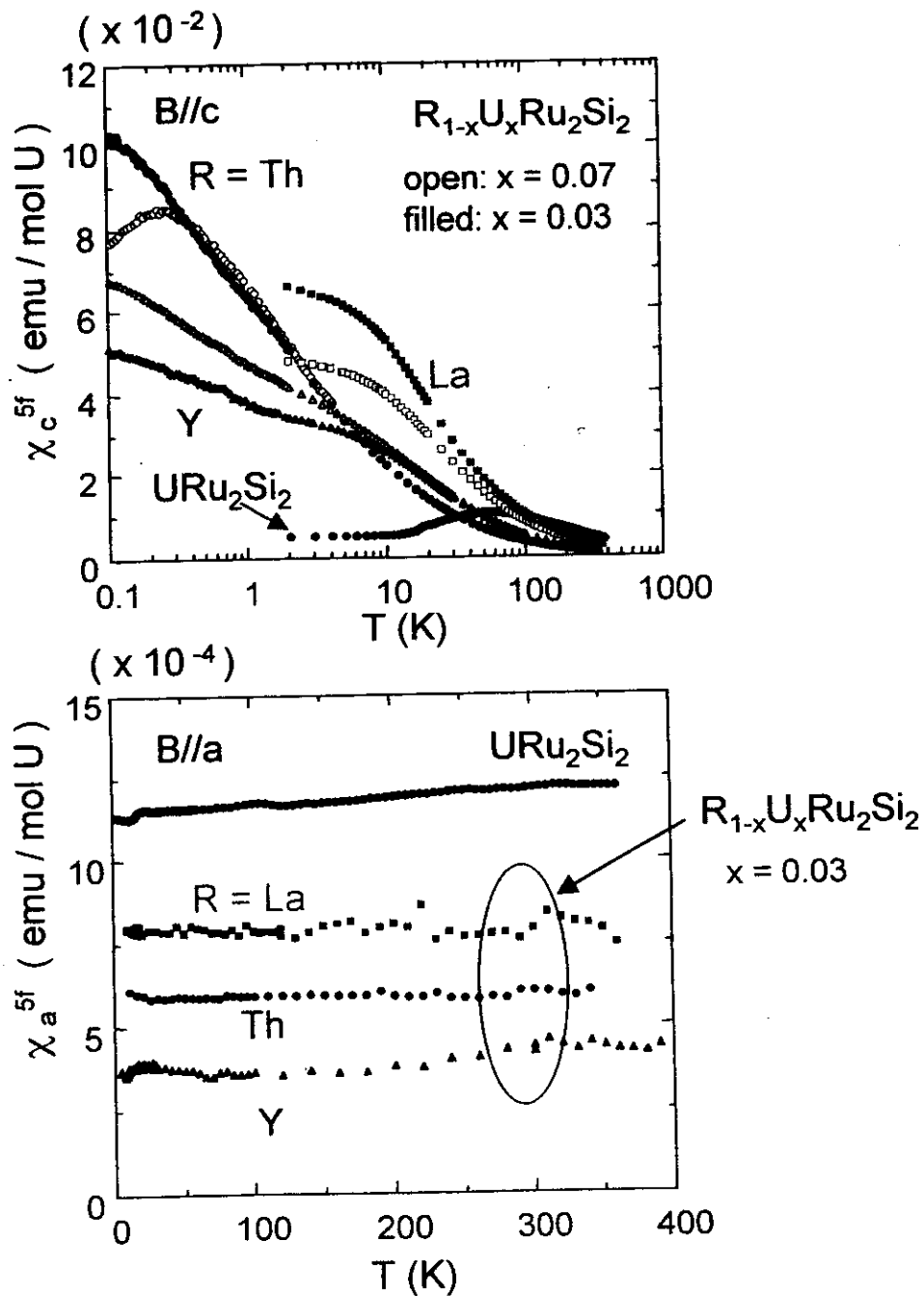
—
 —
 singlet
 $\Gamma_1, \Gamma_2, \text{etc.}$

, or

=
 =
 doublet
 Γ_5

?

$\chi(T)$ in the dilute U limit of URu_2Si_2



Γ_5 non-Kramers doublet

Heavy Electron State at Low-T

$\chi_c \rightarrow \infty$ ($T \rightarrow 0$) in the dilute U limit

Strong Uniaxial Magnetic Anisotropy

$$|\Gamma_5 \pm\rangle = \cos\alpha |\pm 3\rangle + \sin\alpha |\mp 1\rangle = \begin{cases} |\uparrow\rangle \\ |\downarrow\rangle \end{cases}$$

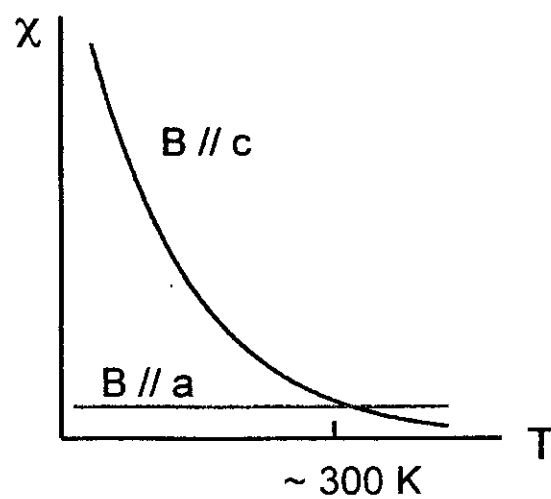
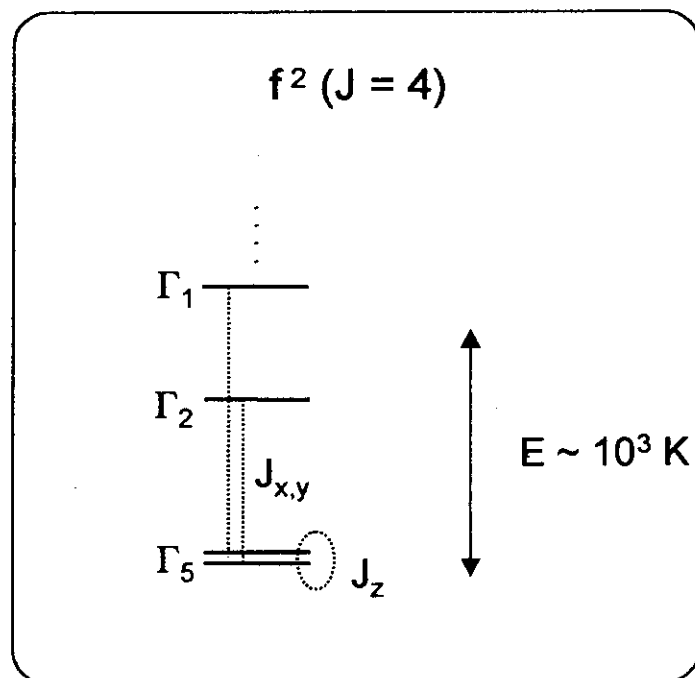
$$J_z \longrightarrow \begin{array}{cc} |\uparrow\rangle & |\downarrow\rangle \\ \left[\begin{array}{c} +g_z \\ -g_z \end{array} \right] \end{array}$$

$$g_z = g_J (3\cos^2\alpha + \sin^2\alpha)$$

$$J_{x,y} \longrightarrow \mathbb{O}$$

$$g_x = g_y = 0$$

A promising CEF scheme with the Γ_5 lowest state



Ohkawa Model

An extended periodic s-d model
with the Γ_5 local state

F.J. Ohkawa and H. Shimizu
J. Phys. 11(1999)L519

$$\begin{array}{lcl}
 O_z = J_z & \longrightarrow & \begin{array}{c} \left[\begin{array}{cc} |\uparrow\rangle & |\downarrow\rangle \\ g_z & -g_z \end{array} \right] \propto S_z \\
 O_{x^2-y^2} = \frac{1}{2}(J_+^2 + J_-^2) \longrightarrow & \begin{array}{c} \left[\begin{array}{cc} & q_1 \\ q_1 & \end{array} \right] \propto S_x \\
 O_{xy} = \frac{-i}{2}(J_+^2 - J_-^2) \longrightarrow & \begin{array}{c} \left[\begin{array}{cc} & -iq_2 \\ iq_2 & \end{array} \right] \propto S_y \end{array} \end{array} \left. \vphantom{\begin{array}{c} \left[\begin{array}{cc} |\uparrow\rangle & |\downarrow\rangle \\ g_z & -g_z \end{array} \right] \propto S_z} \right\} \begin{array}{l} S = \frac{1}{2} \\ \text{pseudo} \\ \text{spin} \end{array} \\
 & & g_x = g_y = 0 \\
 & & g_z \neq 0
 \end{array}$$

$$H_{\text{multi}} = \frac{1}{2} \sum_{\Gamma} \sum_{i,j} A_{\Gamma;ij} O_{\Gamma;i} O_{\Gamma;j}$$



$$H_{\text{spin}} = \frac{1}{2} \sum_{\lambda=x,y,z} \sum_{i,j} J_{\lambda;ij} S_{\lambda;i} S_{\lambda;j}$$

$$H_{\text{eff}} = H_c + H_{sd} + H_{\text{spin}} (+ H_{\text{Zeeman}})$$

Pressure Induced Magnetic Transition

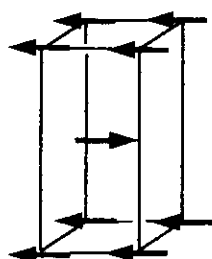
$$P < P_c$$

XY

$$(|J_x| = |J_y| > |J_z|)$$

$$\langle S_z \rangle = 0$$

$$\sqrt{\langle S_x \rangle^2 + \langle S_y \rangle^2} \neq 0$$



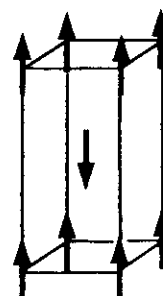
$$P > P_c$$

Ising

$$(|J_x| = |J_y| < |J_z|)$$

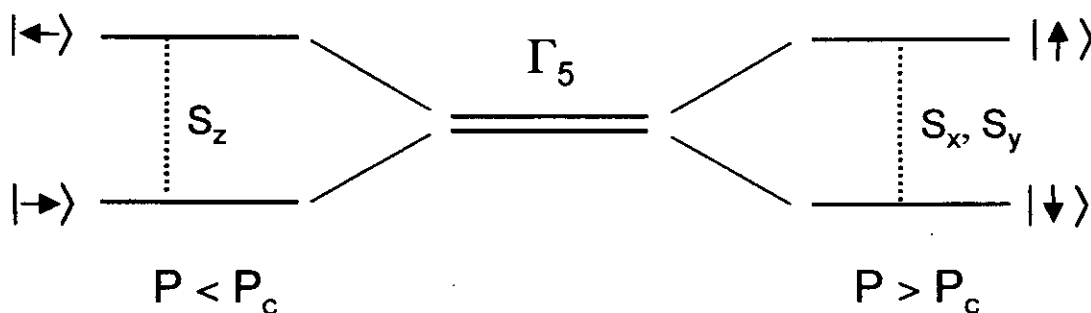
$$\langle S_z \rangle \neq 0$$

$$\sqrt{\langle S_x \rangle^2 + \langle S_y \rangle^2} = 0$$



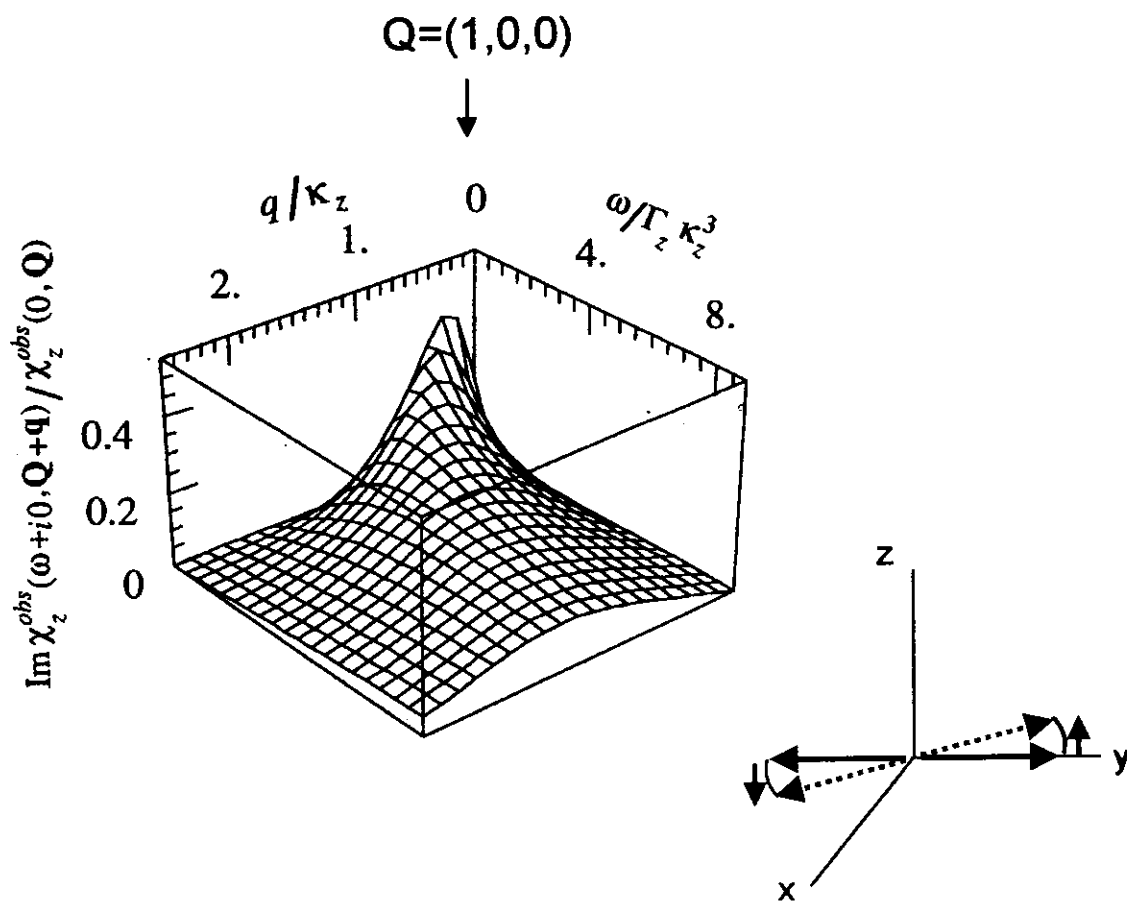
If quadrupolar interactions are dominant

If dipolar interactions are dominant



F.J. Ohkawa and H. Shimizu
J. Phys. 11(1999)L519

The Tiny-Moment AF State



Quantum Spin Fluctuations
Developing under the Pseudo-Spin
Ordered State in the XY Plane

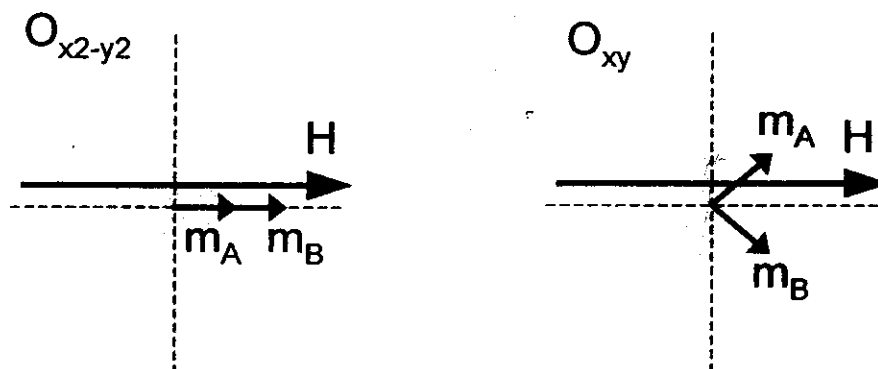
F.J. Ohkawa and H. Shimizu
J. Phys. 11(1999)L519

Advances & Prospects

Observation of the Quadrupole Order

Direct: Resonant X-Ray Scat. ($M_{III} : 5d \rightarrow 5f$)

Indirect: NMR & NSE in Transverse Fields



Time Scale of the AF fluctuation

μ SR

NMR

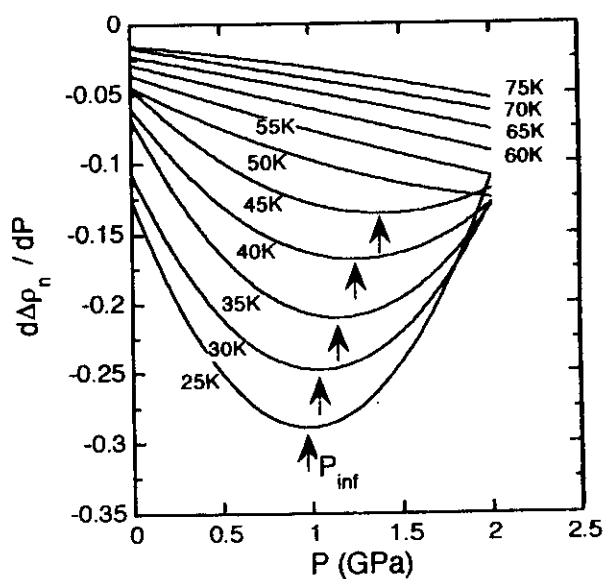
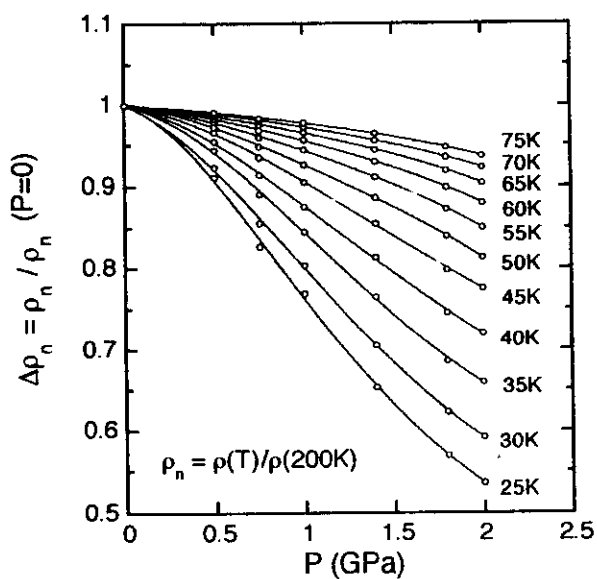
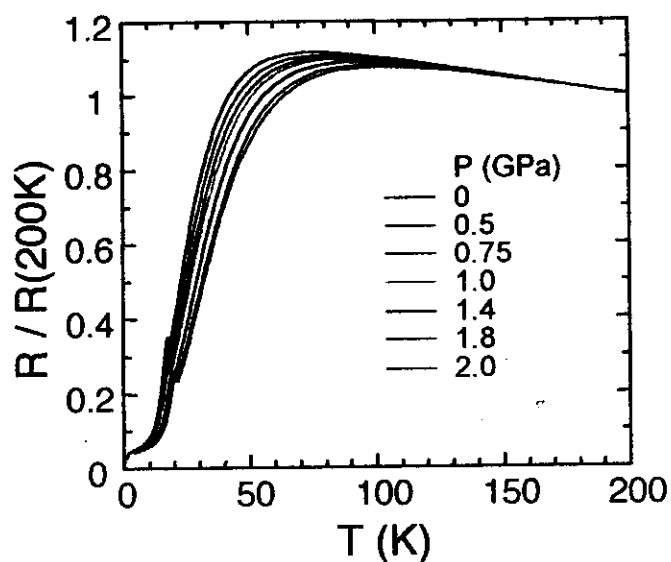
under High P ?

P-T Phase Diagram

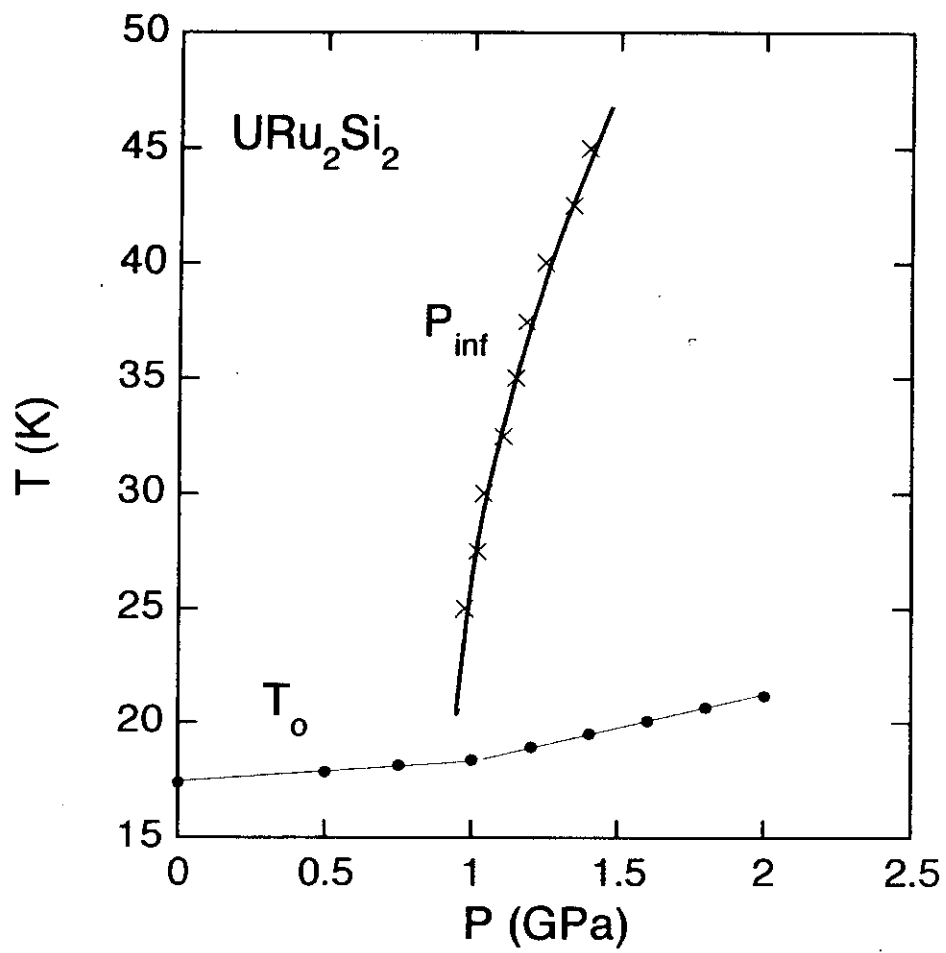
Bulk Measurements,
X-ray Diffraction

$\rho(T)$ under high P

C. Sekine
MIT in Japan

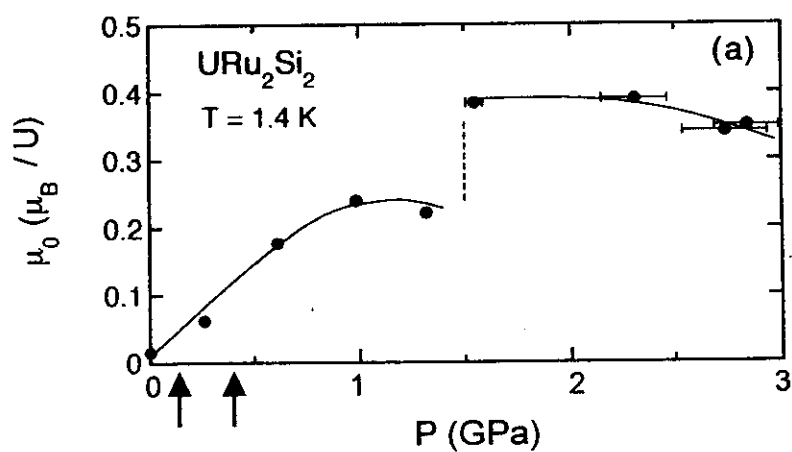
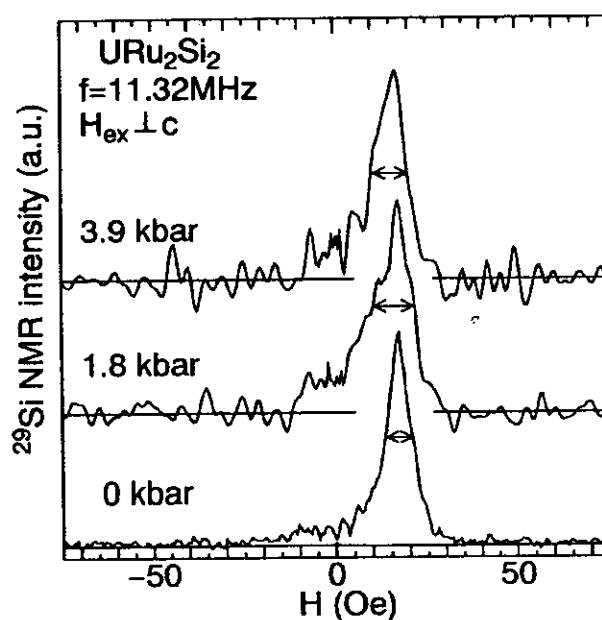


ρ (T) under high P



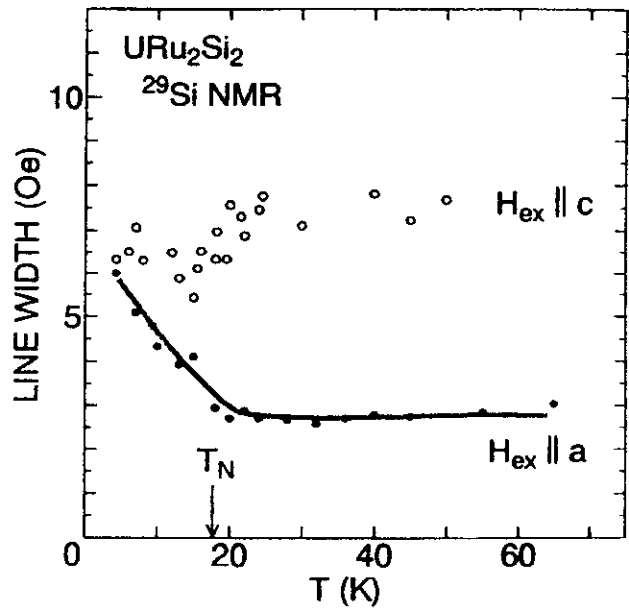
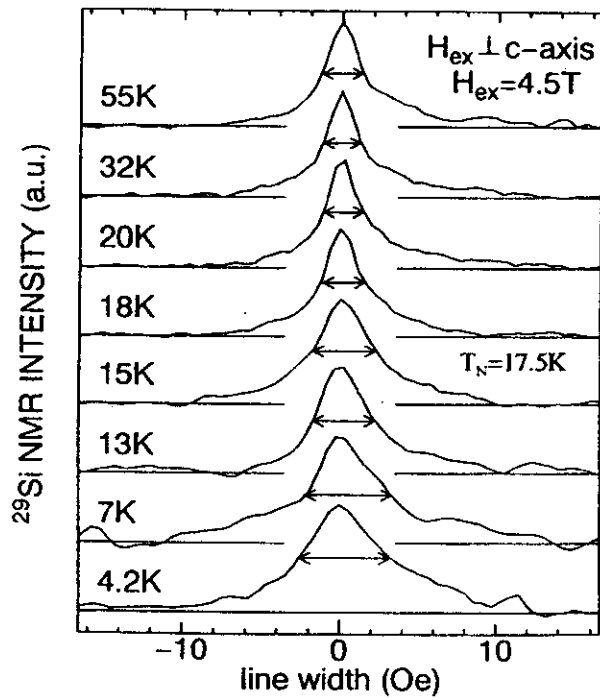
^{29}Si NMR under high P

K. Matsuda
Y. Kohori
T. Kohara

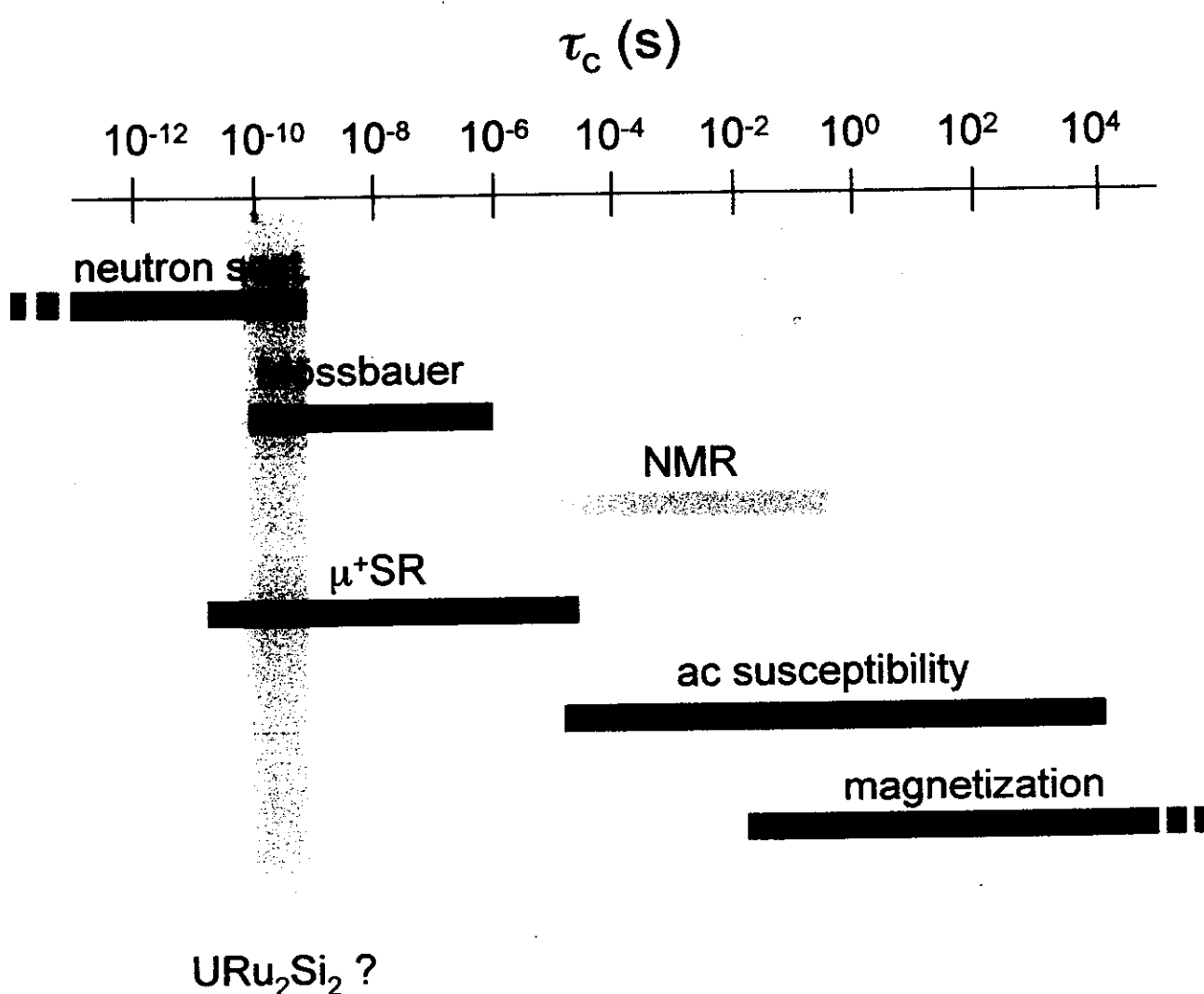


^{29}Si NMR in fields \perp c-axis

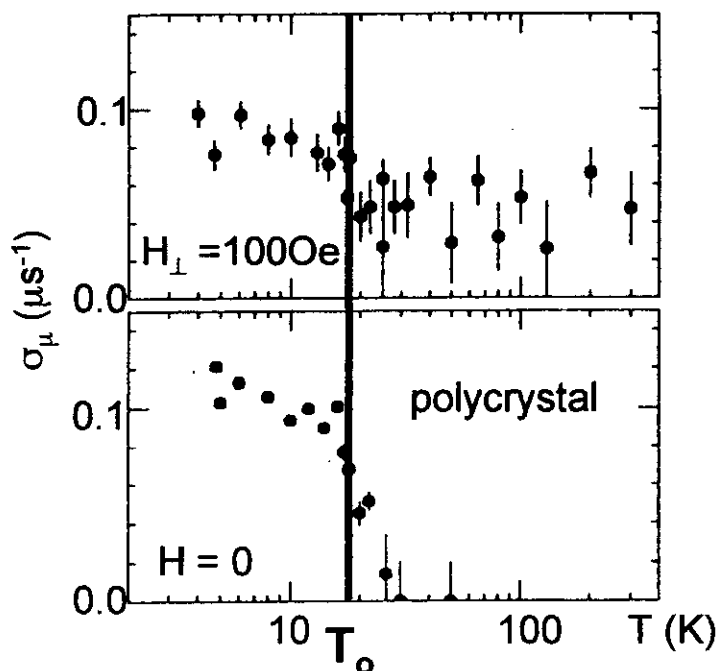
K. Matsuda
Y. Kohori
T. Kohara



Standard time scales of observations for various methods



Previous Reports

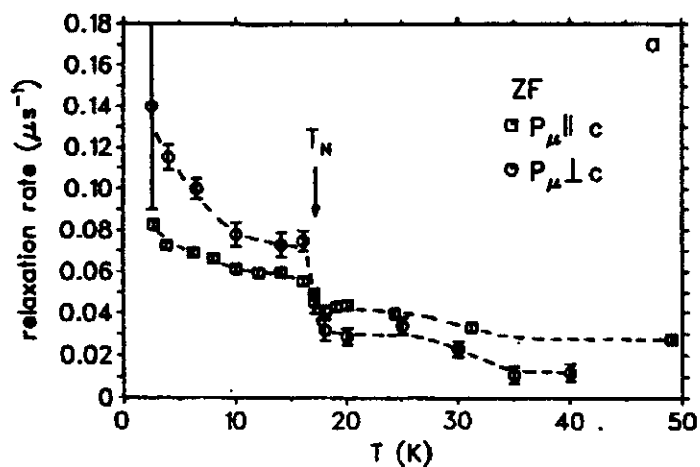


$$\sqrt{\langle H_{\mu}^2 \rangle} \sim 1 \text{ Oe}$$



$$\mu_o \sim 0.001 \mu_B$$

MacLaughlin et al.
PRB37(1988)3153



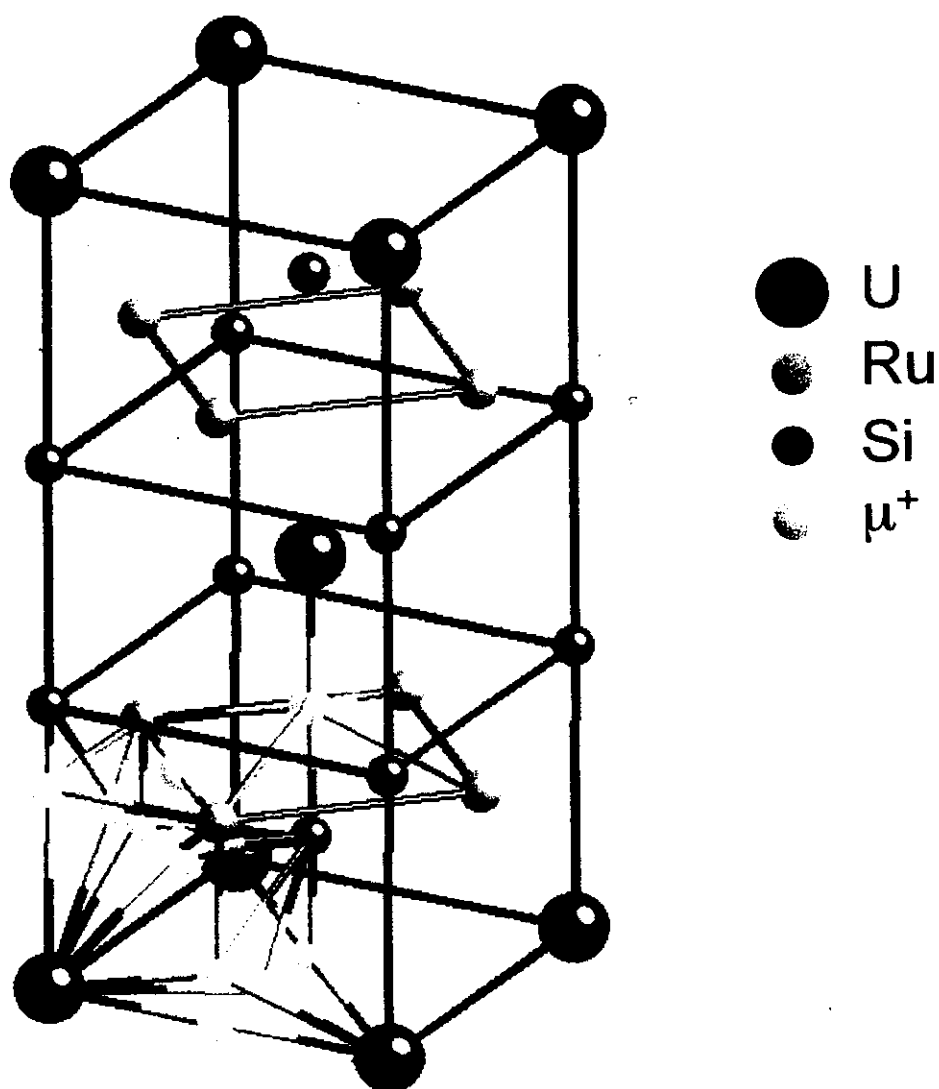
$$\sqrt{\langle H_{\mu}^2 \rangle} \sim 0.2 \text{ Oe}$$



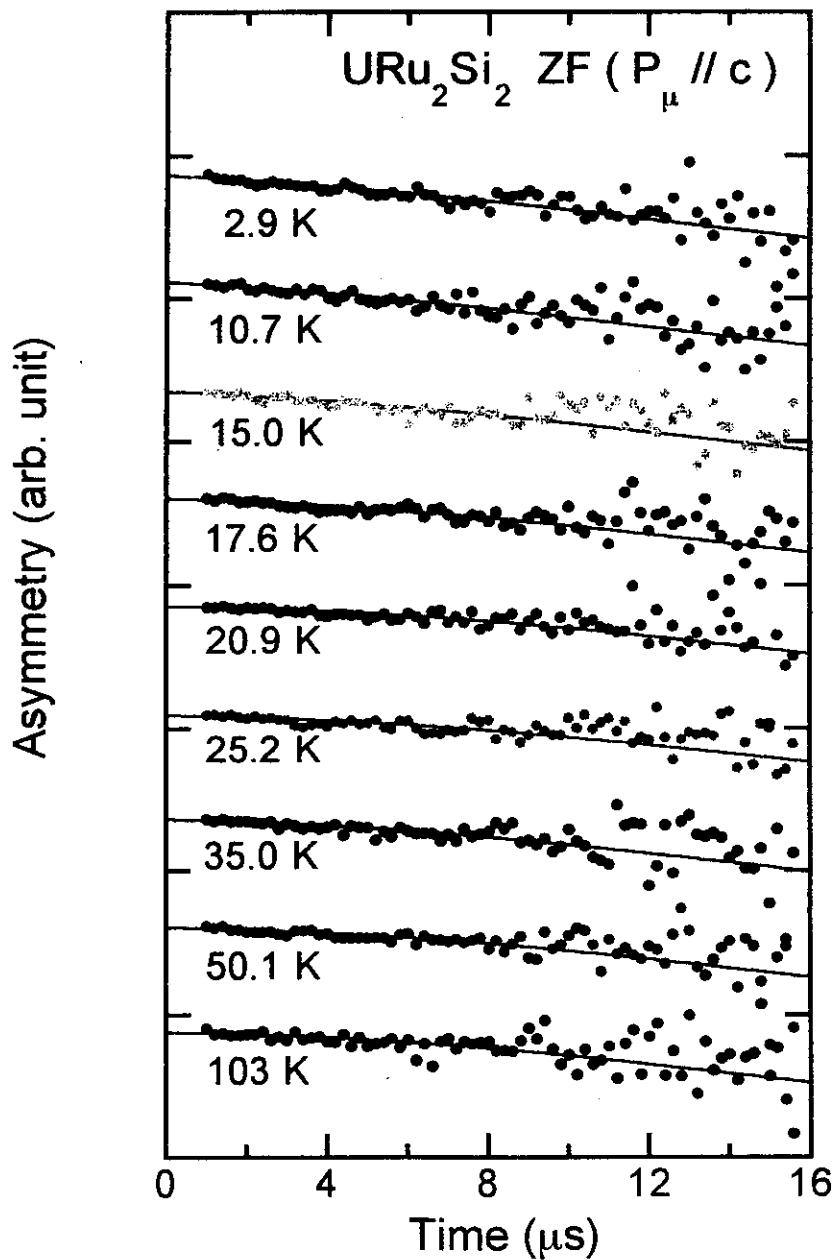
$$\mu_o \sim 0.0002 \mu_B$$

E.A.Knetch et al.
Physica B(1993)300

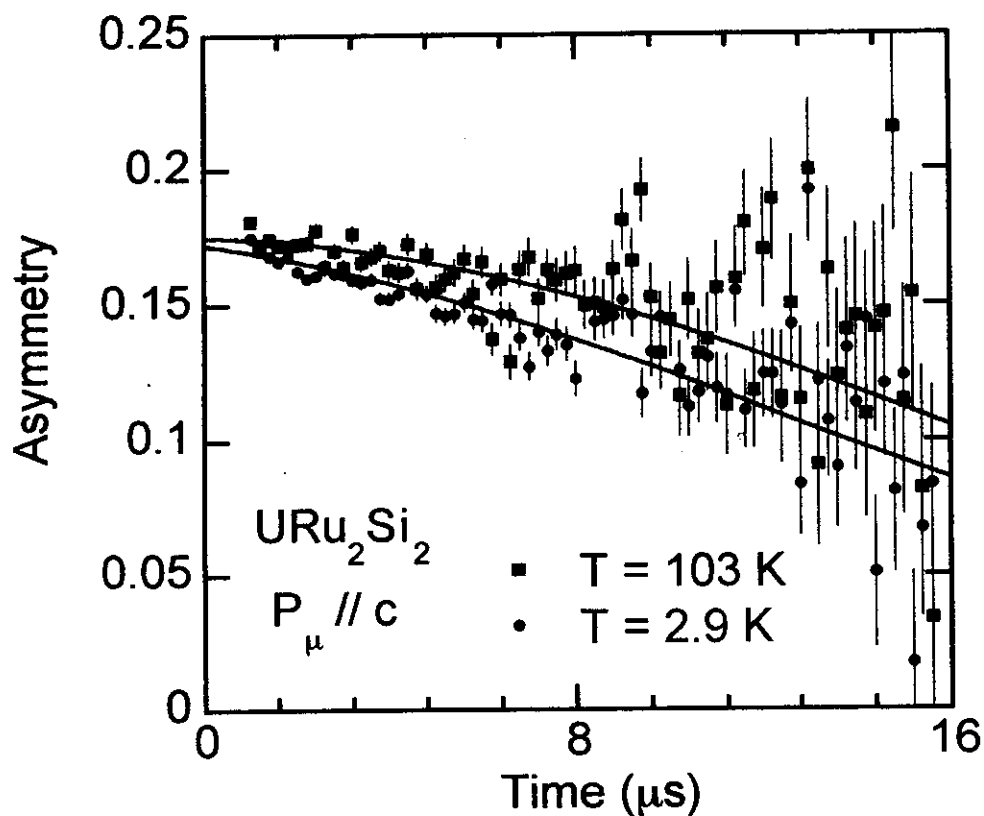
μ^+ stopping sites in URu_2Si_2



T-variations of zero field pulse μ SR spectra of URu_2Si_2



Zero-field pulse μ SR spectra of URu_2Si_2 at 2.9K and 103K



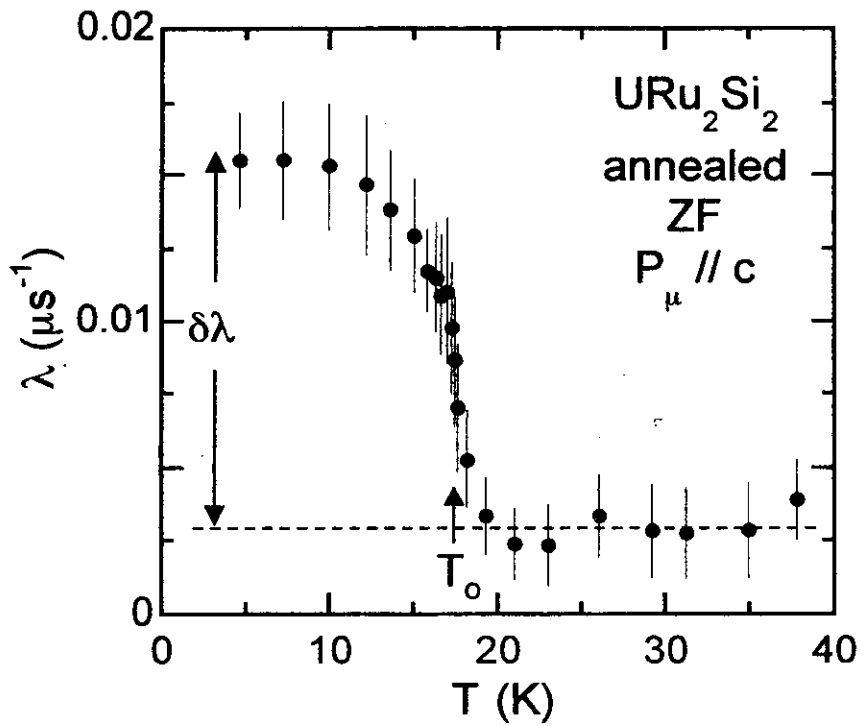
$$G_z(t) = \left\{ \frac{1}{3} + \frac{2}{3} (1 - \sigma_{KT}^2 t^2) \exp\left(-\frac{1}{2} \sigma_{KT}^2 t^2\right) \right\} \exp(-\lambda t)$$

$$\left\{ \begin{array}{l} \text{Kubo-Toyabe function} \\ \text{(nuclear static moments)} \end{array} \right\} \times \left\{ \begin{array}{l} \text{single exponential} \\ \text{(electronic contribution)} \end{array} \right\}$$

$$\sigma_{KT} \sim 0.042 \mu\text{s}^{-1}$$

$$\sqrt{\langle H_\mu^2 \rangle} \sim 0.50 \text{Oe}$$

T-variations of the relaxation rate λ

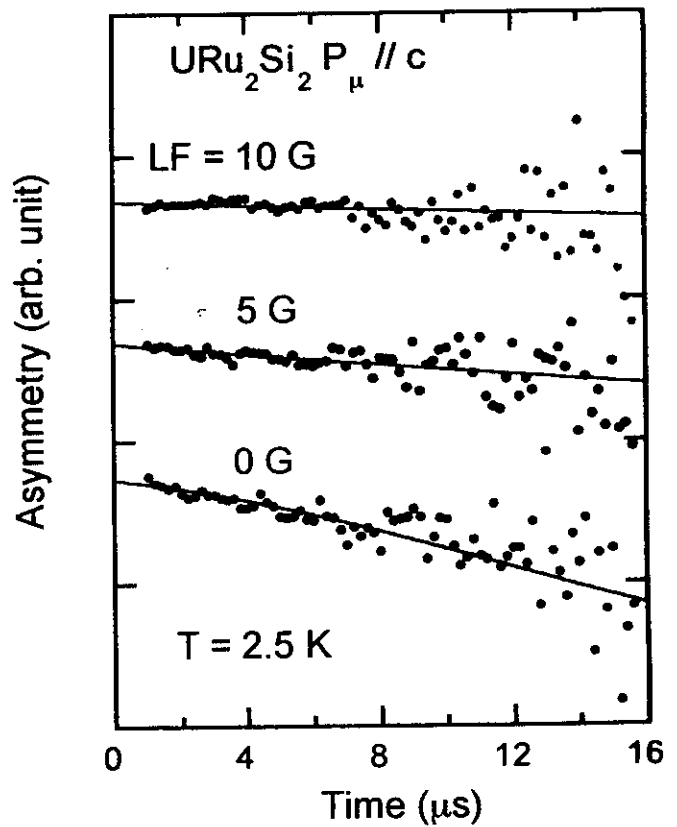
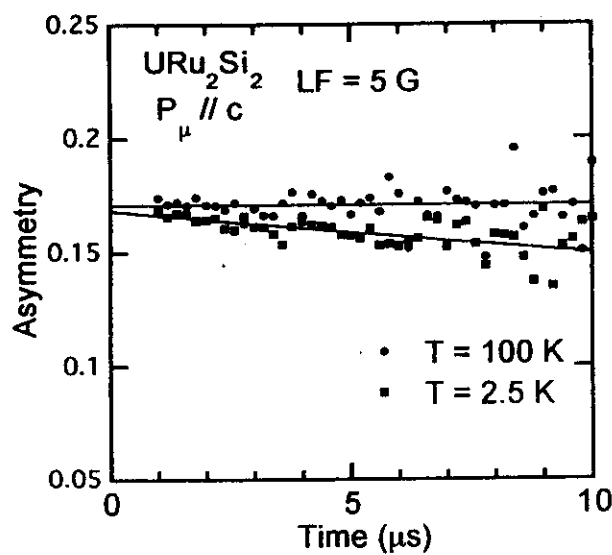


$$\delta\lambda \sim 0.013 \mu\text{s}^{-1}$$

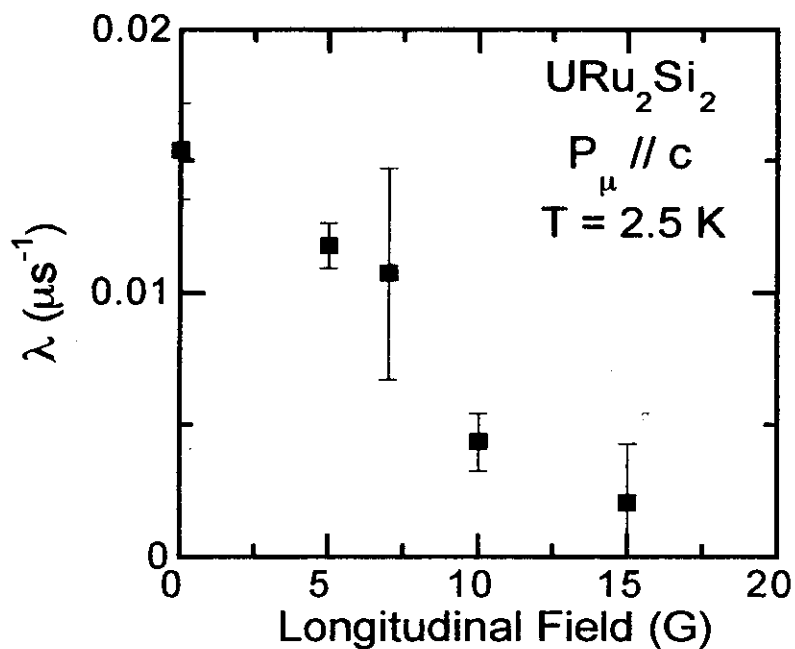
If the μ^+ relaxation is caused by random static fields,

$$\langle H_{\mu} \rangle = \frac{\delta\lambda}{\gamma_{\mu}} \sim 0.15 \text{ Oe.}$$

μ SR spectra in longitudinal fields (Tests of “decoupling”)



μ SR spectra in longitudinal fields (Tests of “decoupling”)



The μ^+ relaxation is caused by dynamical fields.

For fast fluctuations.....

$$\lambda = 2\Delta^2 \tau_c$$

$$\Delta = \gamma_\mu \sqrt{\langle H_\mu^2 \rangle} \sim 100 \text{ (}\mu\text{s}^{-1} \mu_B^{-1}\text{)}$$

$$\mu_o = 0.02 \sim 0.04 \mu_B \text{ (NSE)}$$

$$\tau_c \sim 0.1 - 2 \times 10^{-9} \text{ sec.}$$

